Journal of Catalysis 417 (2023) 74–88

Contents lists available at ScienceDirect

Journal of Catalysis

journal homepage: www.elsevier.com/locate/jcat

Highly efficient and selective partial reduction of nitroarenes to *N*-arylhydroxylamines catalysed by phosphine oxide-decorated polymer immobilized ionic liquid stabilized ruthenium nanoparticles ☆

Reece Paterson [a], Husam Y. Alharbi [a], Corinne Wills [a], Thomas W. Chamberlain [b,*], Richard A. Bourne [b], Anthony Griffiths [b], Sean M. Collins [b], Kejun Wu [b], Matthew D. Simmons [b], Robert Menzel [b], Alexander F. Massey [b], Julian G. Knight [a], Simon Doherty [a,*]

[a] Newcastle University Centre for Catalysis (NUCAT), School of Chemistry, Bedson Building, Newcastle University, Newcastle upon Tyne NE1 7RU, UK
[b] Institute of Process Research & Development, School of Chemistry and School of Chemical and Process Engineering, University of Leeds, Woodhouse Lane, LS2 9JT, UK

ARTICLE INFO

Article history:
Received 13 October 2022
Revised 11 November 2022
Accepted 12 November 2022
Available online 21 November 2022

Keywords:
Polyionic liquid stabilized ruthenium nanoparticles
Highly selective partial reduction of nitroarenes to N-arylhydroxylamines
High turnover frequency
Recycle

ABSTRACT

RuNPs stabilised by a polymer immobilised ionic liquid derived from co-polymerisation of a PEG-substituted imidazolium-based styrene monomer and diphenyl(4-vinylphenyl)phosphine oxide, RuNP@O = PPh_2-PEGPIILS, (**2**) is a remarkably efficient and selective catalyst for the hydrazine hydrate-mediated partial reduction of nitroarenes to the corresponding *N*-arylhydoxylamine. Near quantitative conversion to *N*-phenylhydroxylamine with > 99 % selectivity was obtained after only 2 h when the reaction was conducted at 25 °C in ethanol under an inert atmosphere using 0.1 mol% catalyst. Under these conditions, the composition-time profile showed that the reduction occurred via the direct pathway whereas reactions in air gave a mixture of azoxy-based products due to competing condensation resulting from reversible formation of *N*-phenylhydroxylamine. The initial TOF of 6,100 h^{-1} obtained after 10 min at 40 °C with 0.1 mol% **2** is among the highest to be reported for the metal nanoparticle catalysed reduction of nitrobenzene to *N*-phenylhydroxylamine and a significant improvement on 5 wt% Ru/C which gave a modest conversion of 21 % (initial TOF = 240 h^{-1}) to a mixture of *N*-phenylhydroxylamine and aniline. A broad range of substituted *N*-aryl and *N*-heteroaryl nitroarenes were reduced to the corresponding *N*-arylhydroxylamine in high yield and with excellent selectivity by adjusting the reaction times. However, reduction of electron rich amino-substituted nitroarenes was extremely slow and resulted in reduction to the aniline with no evidence for the corresponding hydroxylamine. Complete reduction of amino substituted nitroarene is proposed to be facilitated by amine-assisted elimination of hydroxide from the hydroxylamine to afford a readily reducible quinondiimine-derived iminium intermediate that reacts with a surface hydride to liberate the amine. Under optimum conditions the catalyst could be reused five times for the reduction of nitrobenzene to *N*-phenylhydroxylamine with no detectable change in activity and only slight decrease in selectivity.

1. Introduction

The synthesis of *N*-arylhydroxylamines is of considerable interest as they are important intermediates to high value products including pharmaceuticals such as acetaminophen and pyraclostrobin and bioactive derivatives of the antibiotics azomycin and chloramphenicol [1–11], fine chemicals [12–14], polymerisation inhibitors [15–16] as well as useful reagents in organic synthesis as they undergo cyclizations, rearrangements and metal-catalysed additions to multiple bonds [17–23]. While *N*-arylhydroxylamines can be prepared by metal catalysed *N*-arylation of a hydroxylamine [24–27] or the catalytic reduction of aldoximines [28–33], the selective reduction of nitroarenes is potentially the most versatile and convenient [34–53]. To this end, while there has been a plethora of reports of the reduction of nitroarenes to the corresponding aniline, selective partial reduction to the thermodynamically unfavourable *N*-arylhydroxylamine remains a challenge. The most common

☆ This article is dedicated to the memory of Professor Stephen A. Westcott, a great ambassador for chemistry and a sincere and genuine friend.

* Corresponding authors.
E-mail addresses: t.w.chamberlain@leeds.ac.uk (T.W. Chamberlain), simon.doherty@ncl.ac.uk (S. Doherty).

https://doi.org/10.1016/j.jcat.2022.11.023
0021-9517/

protocols involve stoichiometric reductions with zinc, tin, antimony or bismuth [34–39] and catalytic reductions using either heterogeneous or nanoparticle-based catalysts such as Rh/C [40–41], Pt/SiO_2 [42], RuNP/CNT [43], RuNP/polystyrene [44], PtNP/Amberlite IRA 900 resin [45], c-PtNP/C [46], IrNP/polystyrene [47], solid-supported PtNP deactivated by DMSO or amine [48–49], silica-supported PdNP [50] and ultra-small palladium nanoclusters [51]. Despite the popularity of this approach, they all suffer one or more drawbacks including, the use of large amounts of expensive noble metal catalyst or stoichiometric quantities of earth abundant metal reagent, the need for an additive, low isolated yields, poor selectivity and functional group tolerance as well as slow rates, the need for harsh reaction conditions and poor environmental credentials due to the use of toxic and/or hazardous reagents and the generation of large amounts of by-product. Recently though, high selectivity for the catalytic reduction of nitrobenzene to *N*-phenylhydroxylamine has been achieved under mild conditions and in good yield using ethylenediamine-modified platinum nanowires [52]. The high selectivity of this system was attributed to an interfacial electronic effect of the modifier as electron donation from the amine rendered the platinum surface electron-rich which favoured adsorption of the electron-deficient nitroarene and disfavoured adsorption of the electron-rich *N*-phenylhydroxylamine. Similarly, high selectivity for the partial reduction of nitrobenzene to *N*-phenylhydroxylamine with perfluoroalkyl-modified cellulose supported ultra-small PdNPs was attributed to the differential absorption of the nitrobenzene and *N*-phenylhydroxylamine caused by a combination of the hydrophobic surface and its electron rich structure [53]. Related reports include solid supported platinum(0) nanoparticles that catalyse the chemoselective reduction of nitroarenes to *N*-arylhydroxylamines using hydrazine hydrate as the hydrogen source [45] and nanoparticulate platinum supported on activated carbon (NanoSelect™) that was highly selective for the *N*-arylhydroxylamine under mild conditions in the presence of the bidentate amine *N,N,N′,N′*-tetramethylethylenediamine (TMEDA) as an additive [46]; the high selectivity of the latter system was proposed to be due to surface substitution of the *N*-arylhydroxylamine by the TMEDA preventing further reduction, however, an interfacial electronic effect of the modifier as described above for platinum nanowires was not considered [51]. To this end, there are an increasing number of reports that the activity and selectivity of nanoparticle-based catalysts can be enhanced by either using organic modifiers to modulate their surface electronic structure and/or steric environment [54–58] or by tuning metal-support interactions [59–60]. For example, the activity and selectivity of Pt, Ru, Rh, Pd and Au nanoparticles as catalysts for hydrogenation can be enhanced in the presence of a σ-donor phosphine or *N*-heterocyclic carbene which act to modulate the surface electronic structure; in many cases the enhancement has been attributed to either the high surface electron density or the ultra-small size of the nanoparticles [61–71]. Other relevant examples include the use of triphenylphosphine cross-linked in the nanopores of the ordered three-dimensional cage-type mesoporous silica FDU-12 to modulate the surface electronic properties of PdNPs and enhance its performance as a catalyst for the hydrogenation of aryl ketones [72] while a phosphine-modified nanoreactor facilitated efficient hydrogenation of benzoic acid over RuNP whereas its unmodified counterpart was inactive; the efficiency of the phosphine modified system was attributed to preferential absorption of the substrate on the electron-rich surface of the nanoparticles, as described for the ethylenediamine modified nanowires discussed above [73]. However, ligand effects are not restricted to phosphine-based donors as amine additives or amine-decorated supports have also been reported to enhance the performance of Pt, Ru Pt/Co and Pd nanoparticles as catalyst for the hydrogenation of carbonyl-based substrates, aromatic compounds and nitroarenes by modifying the surface electronic structure and/or steric properties [66,74–83]. *N*-Heterocyclic carbenes have also been used to modify the surface of Ru, Au, Pd and Pt nanoparticles and improve their performance and stability as catalysts for oxidations and reductions as well as the electrochemical reduction of CO_2 [84–95].

We have recently incorporated heteroatom donors (HAD) into polymer immobilised ionic liquids (PIILs) as supports to stabilise nanoparticles, reasoning that the covalently attached ionic liquid would provide stabilisation through weak electrostatic interactions to the surface of the NP while the heteroatom donor would coordinate to the surface metal atoms and provide additional stabilization to prevent aggregation under the conditions of catalysis [96–104]. In addition, the reports described above suggest that modification of immobilized ionic liquids with a heteroatom donor could also enable the surface electronic structure and steric environment to be modified and/or the size and morphology of the NP to be controlled and, as such, HAD-modified polymer immobilised ionic liquids may well be versatile supports for tuning and optimising catalyst performance [54–95,105]. Our initial endeavours in this area have been extremely promising as PdNPs stabilised by a polyethylene glycol-modified phosphine-decorated PIIL is a remarkably active catalyst for aqueous phase Suzuki-Miyaura cross-couplings [98], the selective hydrogenation of α,β-unsaturated ketones in water [99] and the aqueous phase hydrogenation and transfer hydrogenation of nitroarenes [100], while gold nanoparticles stabilized by a phosphine oxide-decorated polymer immobilised ionic liquid is a highly efficient and selective catalyst for the partial reduction of nitrobenzene to either *N*-phenylhydroxylamine or azoxybenzene and complete reduction to aniline [101]. Our most recent endeavours in this area have revealed that ruthenium nanoparticles stabilized by the same polymer is a remarkable efficient catalyst for the hydrogenation of aryl and heteroaryl ketones to the corresponding alcohol and levulinic acid to γ-valerolactone [102] as well as the hydrolytic evolution of hydrogen from sodium borohydride [103–104]. Herein, we report that RuNP stabilised by a phosphine oxide-decorated polymer immobilised ionic liquid catalyses the partial reduction of a wide range of nitroarenes in ethanol under mild condition and with remarkable efficiency to afford high yields of the corresponding *N*-arylhydroxylamine with exceptional selectivity (>99 %); in stark contrast, the corresponding AuNP-based system catalyses the sodium borohydride-mediated reduction of nitrobenzene in

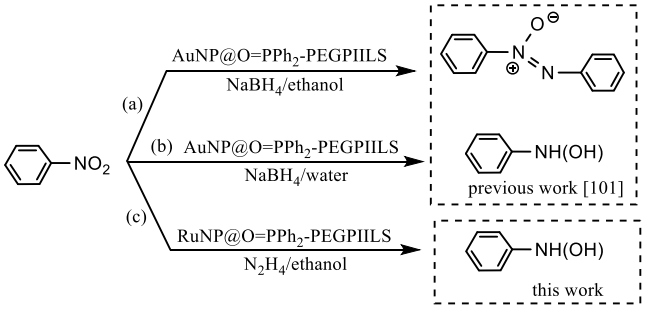

Scheme 1. Selective partial reduction of nitrobenzene with AuNP@O = PPh_2-PEGPIILS and RuNP@O = PPh_2-PEGPIILS; both catalysts are generated by sodium borohydride-mediated reduction of the corresponding metal chloride loaded precursor [$AuCl_4$]@O = PPh_2-PEGPIILS, and [$RuCl_3$]Cl@O = PPh_2-PEGPIILS, respectively. (a) Reaction conducted in ethanol and catalysed by AuNP@O = PPh_2-PEGPIILS to afford azoxybenzene, (b) reaction conducted in water and catalysed by AuNP@O = PPh_2-PEGPIILS to afford *N*-phenylhydroxylamine and (c) reaction conducted in ethanol and catalysed by RuNP@O = PPh_2-PEGPIILS to afford *N*-phenylhydroxylamine.

ethanol to give quantitative conversion to azoxybenzene as the sole product (Scheme 1).

In addition to this remarkable metal-dependent switch in selectivity, the RuNP-based catalyst described herein is unrivalled in its efficiency as a catalyst for the selective reduction of nitroarenes to the corresponding *N*-arylhydroxylamine as it operates under mild conditions, gives high yields and near quantitative selectivity in short reaction times with a low catalyst loading and reactions are conducted in a green and sustainable solvent [106]; in addition, the catalyst can be reused up to 5 times with only minor changes in conversion and selectivity. While ruthenium nanoparticles on carbon nanotubes have previously been reported to catalyse the hydrazine-mediated selective reduction of nitroarenes to the *N*-arylhydroxylamine and aniline, THF was required to achieve high selectivity for partial reduction to the hydroxylamine whereas reactions conducted in alcohol were unselective and gave a mixture of the *N*-arylhydroxylamine and aniline; moreover, TOFs were also significantly lower, and reactions were conducted with a large excess of reducing agent [43]. High selectivity for the partial reduction of nitroarenes to the hydroxylamine has also been reported with polymer-supported RuNPs, although reactions had to be conducted in either chloroform or THF as the use of methanol and ethanol gave low conversions to a mixture of the *N*-arylhydroxylamine and the corresponding aniline [44].

2. Results and discussion

2.1. Catalyst synthesis and characterisation

The phosphine oxide-decorated polymer immobilised ionic liquid **1** required for this study was prepared by AIBN-initiated polymerisation of the corresponding PEG-substituted imidazolium based monomer, imidazolium cross-linker and diphenyl(4-vinyl phenyl)phosphine oxide in a ratio of x = 1.84, y = 1.0, z = 0.16, as previously described [98–99]. Catalyst **2** was prepared by wet impregnation of **1** with ruthenium trichloride to afford a precursor with a ruthenium to phosphine oxide ratio of one; this was then reduced *in situ* with an excess of $NaBH_4$ to afford RuNP@O = PPh_2-PEGPIILS (**2**), which was isolated in good yield as a free-flowing black powder after work-up (Fig. 1). The catalyst was characterised by a combination of solid-state NMR spectroscopy, IR spectroscopy, SEM, TEM, EDX and XPS and the ruthenium loading was determined by ICP-OES. The solid state ^{13}C CP/MAS NMR spectrum of **2** is entirely consistent with the target formulation and contains a characteristic set of resonances between δ 122 and 145 ppm for the imidazolium ring, the aromatic carbon atoms of the styrene and the phenyl groups of the diphenyl-phosphine oxide, signals between δ 10 and 51 ppm associated with the methylene and methine carbon atoms of the polystyrene backbone and the methyl group attached to the imidazolium ring and resonances at δ 70 and 58 ppm belonging to the methylene carbon atoms of the PEG chain and the terminal OMe, respectively.

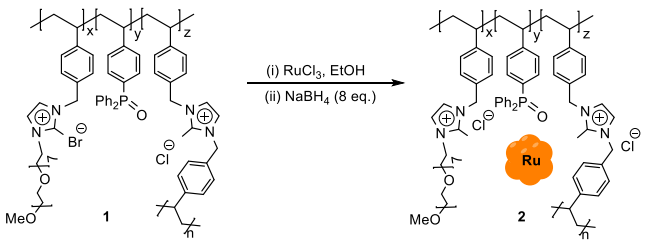

Fig. 1. Synthesis and composition of PIIL-stabilised ruthenium nanoparticles **2**.

TEM micrographs of **2** revealed that the ruthenium nanoparticles were ultrafine and near monodisperse with an average diameter of 2.30 ± 0.57 nm (Fig. 2a) and EDX elemental mapping (Fig. 2b) revealed an even distribution and good dispersity of the RuNPs within the support. SEM images revealed that the catalyst material was far more granular than its polymeric counterpart, which appeared largely smooth. The surface of catalyst **2** was characterised by X-ray photoelectron spectroscopy (XPS) by analysing the Ru 3p region because of overlap of the C 1s and Ru 3d region. XPS clearly evidences the presence of Ru in the sample. The atomic Ru concentration, detectable by XPS, is relatively small at around 0.25 at%. Considering the pronounced surface sensitivity of XPS, this small detectable concentration value suggests that the Ru nanoparticles are extremely well integrated into the polymer matrix, rather than phase-separating on the sample surface. The high-resolution spectrum shows two characteristic Ru 3p XPS peaks at 463.5 eV and 486.3 eV. These peak positions are significantly up-shifted compared to reported peak positions for metallic Ru(0) (461.3 eV and 483.5 eV)[1], suggesting the presence of Ru(IV) within the sample (reported peak positions for Ru(IV): 463.0 eV and 485.2 eV) [107].

2.2. Selective reduction of nitroarenes to N-arylhydroxylamines

The catalytic reduction of nitroarenes was initially targeted to compare the efficacy of **2** against its AuNP counterpart, as the latter is a highly selective solvent dependent catalyst for the partial reduction of nitroarenes to the corresponding *N*-arylhydroxylamine in water but switched selectivity to azoxyarene in ethanol (Scheme 1). Our initial investigations focused on the reduction of nitrobenzene as this is the accepted benchmark substrate to screen newly developed catalysts and its reduction has been catalysed by nanoparticles stabilised with various supports [108–109] including: carbon nanotubes [43], rutile or anatase [110–111], phosphine-functionalised ionic liquid [62–63], PVP [112–116], dendrimers [117–118], bulky amphiphilic PEG-based tripodal ligands [119], fullerene C_{60} [80,120] porous polymers [121], carbon nitride [122] and carbon nanosphere [123]. A preliminary reaction conducted in ethanol at 40 °C under nitrogen using 0.1 mol% **2** and three mole equivalents of hydrazine hydrate gave 94 % conversion and > 98 % selectivity for *N*-phenylhydroxylamine after only 30 min with an initial TOF of 6,100 mol product mol $Ru^{-1}h^{-1}$; under these conditions azoxybenzene (<2 %) was identified as the only other product (Table 1, entry 1). At this stage, we are confident that the minor amount of azoxybenzene that appears in the ^1H NMR spectrum is formed when the sample is briefly exposed to air during the aqueous work-up and that the formation of *N*-phenylhydroxylamine is irreversible when the reaction is conducted under a nitrogen atmosphere (see later). The solvent dependent selectivity of its gold-nanoparticle counterpart, AuNP@O = PPh_2-PEGPIILS, prompted us to first undertake a survey of the performance of **2** in a range of solvents. Table 1 reveals that good conversions and high selectivities for *N*-phenylhydroxylamine were also obtained in methanol and THF and while high conversions were also obtained in toluene and a 1:1 mixture of ethanol and water the selectivities were significantly lower due to complete reduction to aniline (Table 1, entries 2–5). When the reaction was conducted in water the conversion only reached 44 % at the same time with 46 % selectivity for *N*-phenylhydroxylamine and 54 % selectivity for aniline (Table 1, entry 6); this is in stark contrast to the corresponding AuNP-based system which catalysed the sodium borohydride-mediated reduction of nitrobenzene in water with quantitative conversion to *N*-phenylhydroxylamine [101]. A more detailed study of the catalyst performance as a function of the ethanol–water composition revealed that the selectivity dropped to 64 % in a 5:1 mixture of

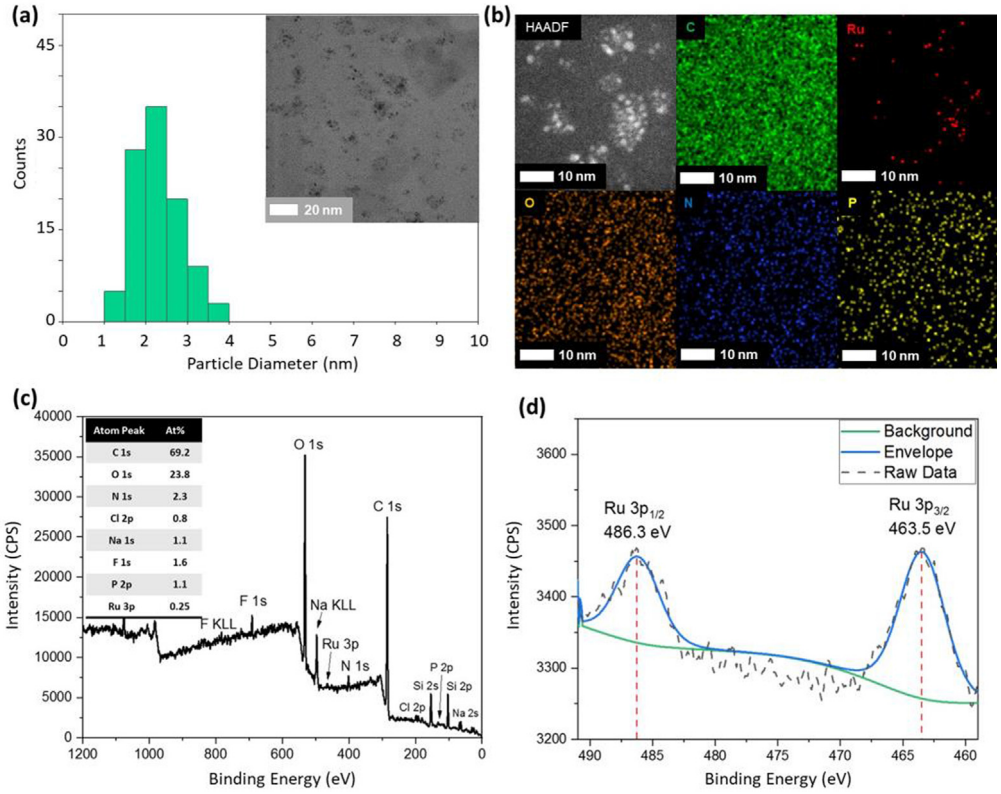

Fig. 2. (a) HRTEM image of **2** (inset) and corresponding size distribution determined by counting > 100 particles. Scale bars are 20 nm; (b) HAADF image (grey) and individual EDX elemental maps for **2**, showing; C (green), Ru (red), O (orange), N (blue) and P (yellow). Scale bars are 10 nm (white). (c) XPS survey spectrum of **2** (inset shows elemental surface composition in at%) and (d) high-resolution Ru 3p XPS spectrum of **2**. (For interpretation of the references to colour in this figure legend, the reader is referred to the web version of this article.)

Table 1
Selective partial reduction of nitrobenzene to *N*-phenylhydroxylamine as a function of catalyst, solvent, temperature, and hydride source.[a].

Entry	Catalyst (mol %)	Hydride (equiv.)	Temp (°C)	solvent	Time (min)	Conv. (%) [b]	Selectivity (%) [c]		
							N-PHA	AZOXY	Aniline
1	**2** (0.1)	N_2H_4 (3)	40	EtOH	60	100	98	2	–
2	**2** (0.1)	N_2H_4 (3)	40	MeOH	60	89	94	1	5
3	**2** (0.1)	N_2H_4 (3)	40	THF	60	100	89	2	9
4	**2** (0.1)	N_2H_4 (3)	40	Toluene	60	97	56	2	42
5	**2** (0.1)	N_2H_4 (3)	40	EtOH/H_2O	60	100	82	1	17
6	**2** (0.1)	N_2H_4 (3)	40	H_2O	60	44	46	–	54
7	**2** (0.1)	N_2H_4 (2)	40	EtOH	60	62	94	2	4
8	**2** (0.1)	N_2H_4 (1)	40	EtOH	60	27	90	3	7
9	**2** (0.1)	N_2H_4 (10)	40	EtOH	60	100	84	1	15
10	**2** (0.1)	$NaBH_4$ (3)	40	EtOH	60	100	71	20	9
11	**2** (0.1)	$NaBH_4$ (3)	40	H_2O	60	29	12	6	82
12	**2** (0.1)	DMAB (3)	40	EtOH	60	6	56	0	44
13	**2** (0.1)	HCO_2H (3)	40	EtOH	60	0	–	–	–
14	**2** (0.1)	N_2H_4 (3)	50	EtOH	60	100	88	2	10
15	**2** (0.1)	N_2H_4 (3)	60	EtOH	60	100	70	2	28
16	**2** (0.1)	N_2H_4 (3)	25	EtOH	60	68	>99	<1	–
17	**2** (0.1)	N_2H_4 (3)	25	EtOH	120	100	>99	<1	–
18	**2** (0.05)	N_2H_4 (3)	40	EtOH	60	74	97	2	–
19	**2** (0.2)	N_2H_4 (3)	40	EtOH	60	100	93	1	6
20	Ru/C (0.1)	N_2H_4 (3)	25	EtOH	120	21	76	4	12
21	AuNP (0.1)	N_2H_4 (3)	25	EtOH	120	0	–	–	–
22	PtNP (0.1)	N_2H_4 (3)	25	EtOH	120	56	91	4	5
23	PtNP (0.1)	N_2H_4 (3)	25	H_2O	120	74	89	2	9

[a] Reaction conditions: Conducted under nitrogen, 1 mmol nitrobenzene, mol% catalyst, 2 mL solvent, hydride source, time, temperature. [b] % Conversion determined by ^1H NMR spectroscopy using 1,4-dioxane as internal standard. Average of at least three runs. [c] Selectivity for *N*-phenylhydroxylamine [% *N*-phenylhydroxylamine / (% *N*-phenylhydroxylamine + % azoxybenzene + % azobenzene + % aniline)] × 100%.

ethanol and water; interestingly, the selectivity improved slightly to 86 % when the volumetric ratio was increased to 1:2 and then dropped again to 77 % in a 1:5 mixture of ethanol and water and ultimately to 54 % in neat water (see Figure S1 in the supporting information for full details). In this regard, there have been several related reports of solvent dependent selectivity profiles for the

metal nanoparticle catalysed reduction of nitrobenzene to *N*-phenylhydroxylamine. Particularly relevant examples include the hydrazine hydrate-mediated reduction of nitrobenzene catalysed by RuNP on carbon nanotubes which gave *N*-phenylhydroxylamine in 97 % yield in THF whereas the selectivity switched to afford aniline as the sole product in water [43]. The same reaction catalysed by polystyrene-stabilised RuNPs gave complete conversion with 96 % selectivity for *N*-phenylhydroxylamine in chloroform but only reached 69 % conversion to a 1:1 mixture of *N*-phenylhydroxylamine and aniline in ethanol [44]. Other examples include the palladium nanocluster-catalysed sodium borohydride-mediated reduction of nitrobenzene which gave a very low conversion (<10 %) in water but complete conversion with an optimum selectivity of 97 % for *N*-phenylhydroxylamine in a mixture of water and ethanol; interestingly, the selectivity decreased quite dramatically as the solvent mixture was varied [51]. Finally, the solid-supported PtNP catalysed hydrazine hydrate-mediated selective reduction of nitrobenzene gave a near quantitative conversion to *N*-phenylhydroxylamine in PEG-400 compared with only 40 % in water [45].

The high selectivity obtained in ethanol and its environmentally benign and sustainable credentials prompted us to perform the remainder of our optimisation studies and substrate screening in this solvent. As a large excess of reducing agent is often used for the reduction of nitroarenes (>10 equivalents) the conversion and selectivity profile was investigated as a function of the N_2H_4 to nitrobenzene mole ratio (Table 1, entries 7–9). The conversion dropped quite dramatically from 100 % with three equivalents of N_2H_4 to 62 % with two equivalents and only 27 % with one equivalent, under otherwise identical conditions. Not surprisingly, complete conversion was also obtained when the ratio was increased to 5 and 10 equivalents, however, the selectivity dropped to 84 % due to the formation of aniline and as such all further studies were conducted with three mole equivalents of hydrazine hydrate since this ratio gave complete conversion with high selectivity in a relatively short reaction time (1 h); moreover, the use of only a slight excess of reducing agent also improves the overall reagent efficacy of the process. Variation of the hydrogen donor revealed that hydrazine hydrate gave the optimum combination of conversion and selectivity for reductions conducted in ethanol, as $NaBH_4$ gave quantitative conversion to a mixture of *N*-phenylhydroxylamine, azoxybenzene and aniline after 1 h with 71 % selectivity for *N*-phenylhydroxylamine (Table 1, entry 10); a very similar selectivity profile was also obtained at 55 % conversion when the reaction time was reduced to 10 min suggesting that the complete reduction is facile under these conditions. In order to directly compare the efficacy of **2** against its AuNP counterpart, which gave complete conversion to *N*-phenylhydroxylamine as the sole product in water with $NaBH_4$ as the reducing agent, the same reduction was catalysed by 0.1 mol% **2** in water at 25 °C with three equivalents of $NaBH_4$. Surprisingly, under these conditions, the reaction only reached 29 % conversion after 1 h with 82 % selectivity for aniline (Table 1, entry 11), which emphasises that the kinetics of this consecutive multi-step reduction are complicated and dependent on the combination of metal, reducing agent and solvent. Other common reducing agents such as NMe_2HBH_3 and formic acid triethylamine azeotrope gave negligible conversions under the same conditions (Table 1, entries 12–13). Hydrazine hydrate has been reported to be the hydrogen donor of choice for the catalytic reduction of nitroarenes with nanoparticles. For example, polystyrene supported IrNPs [47], carbon nanotubes RuNP nanohybrids [43], polystyrene supported ruthenium nanoparticles [44], solid supported PtNPs [45], carbon nitride supported PdNPs [122], PdNP immobilised on carbon nanospheres [123], polystyrene immobilised RuCoNPs [124] and bimetallic PdAuNPs immobilised on TiO_2 [125].

A survey of the effect of the temperature revealed that the selectivity for *N*-phenylhydroxylamine decreased with an increase in the reaction temperature due to the formation of aniline. For example, when the reduction was conducted with three equivalents of hydrazine hydrate in ethanol at 50 °C using 0.1 mol% **2**, *N*-phenylhydroxylamine was obtained in 88 % yield and selectivity together with 11 % aniline and a trace amount of azoxybenzene after 1 h; a further increase in the reaction temperature to 60 °C gave 70 % *N*-phenylhydroxylamine and 28 % aniline (Table 1, entries 14–15). When the reaction temperature was reduced to 25 °C the high selectivity for *N*-phenylhydroxylamine (>99 %) was retained but the conversion dropped to 65 % after 1 h with an initial TOF of 1,040 mol product mol $cat^{-1}h^{-1}$; gratifyingly though, complete conversion was obtained by increasing the reaction time to 2 h (Table 1, entry 16–17). A similar temperature dependent selectivity profile for the platinum nanoparticle catalysed reduction of nitrobenzene has previously been reported such that high selectivity for *N*-phenylhydroxylamine was obtained below 30 °C while aniline and *N*-phenylhydroxylamine formed at similar rates above 60 °C [46]. Thus, aniline can also be obtained as the sole product using 0.1 mol% of catalyst **2** simply by increasing the reaction temperature and/or time appropriately (see later). A brief survey of the catalyst loading confirmed that the optimum selectivity and conversion was obtained with 0.1 mol% **2** as an increase in the catalyst loading to 0.2 mol% resulted in complete conversion after 1 h at 40 °C but with a slight drop in selectivity to 93 % due to formation of aniline (Table 1 entry 18–19) while a reduction in the catalyst loading to 0.05 mol% resulted in a concomitant reduction in conversion to 84 % after 2 h, albeit with 98 % selectivity for *N*-phenylhydroxylamine. As reactions conducted with 0.1 mol% catalyst gave the optimum combination of conversion and selectivity after only 2 h at 25 °C, this loading was used for substrate screening and further catalytic studies.

A comparison of the efficacy of **2** as a catalyst for the selective partial reduction of nitrobenzene to *N*-phenylhydroxylamine against other NP-based catalysts revealed that **2** is among the most active. For example, the initial TOF of 8,760 mol product mol $cat^{-1}h^{-1}$ obtained with **2** at 40 °C is substantially higher than the 61 mol product mol $cat^{-1}h^{-1}$ obtained with solid supported PtNPs at 60 °C [45], 830 mol product mol $cat^{-1}h^{-1}$ obtained in THF at room temperature with RuNPs supported on carbon nanotubes [43], 234 mol product mol $cat^{-1}h^{-1}$ for polystyrene-supported RuNP [44], and a substantial improvement on that of 87 mol product mol $cat^{-1}h^{-1}$ for polystyrene stabilised IrNPs at 85 °C [47], 200 mol product mol $cat^{-1}h^{-1}$ for 5 wt% Pt/SiO_2 [48] but lower than the 13,943 mol product mol $cat^{-1}h^{-1}$ reported for activated carbon supported platinum nanoparticles [46]. The efficacy of **2** was also compared with commercially available 5 mol% Ru/C (Alfa Aesar, Ruthenium, 5 % on activated carbon powder 11748) and, under otherwise identical conditions, 0.1 mol% Ru/C catalysed this reduction but only reached 21 % conversion to a mixture of aniline (12 %) and *N*-phenylhydroxylamine (76 %) after 2 h (Table 1, entry 20). To this end, a modest conversion and poor selectivity for *N*-phenylhydroxylamine has previously been reported for commercially available 5 % Ru/C [44]. Finally, a control reaction for the reduction of nitrobenzene conducted at 40 °C in ethanol under nitrogen with three equivalents of hydrazine hydrate but in the absence of catalyst gave no conversion even after 5 h, confirming that RuNPs were essential for the catalytic reduction.

The high selectivity and yield of *N*-phenylhydroxylamine obtained from the sodium borohydride-mediated reduction of nitrobenzene in water with AuNPs stabilised by a phosphine oxide decorated polymer immobilised ionic liquid as the catalyst prompted us to explore its efficacy using hydrazine hydrate as the reducing agent to compare the selectivity with its RuNP counterpart. Interestingly, negligible conversions were obtained in

either water, ethanol or a 1:1 mixture of water and ethanol after 2 h at 25 °C using 0.1 mol% AuNP@O = PPh_2-PEGPIILS and three equivalents of hydrazine hydrate (Table 1, entry 21), which highlights the importance of identifying an optimum combination of the metal nanoparticle and reducing agent. A comparison of the performance of **2** against PtNP@PPh_2-PEGPIILS was also undertaken as there have been several reports of efficient and selective hydrogenation or reduction of nitrobenzene to *N*-phenylhydroxylamine including solid supported PtNPs [45], ethylenediamine coated platinum nanowires [52], and Pt/C deactivated with either DMSO or DMSO and triethylamine [48–49,126]. Under the optimum conditions described above, the hydrazine hydrate-mediated reduction of nitrobenzene catalysed by 0.1 mol % PtNP@PPh_2-PEGPIILS gave 56 % conversion in ethanol with 91 % selectivity for *N*-phenylhydroxylamine while the conversion increased to 74 % in water with 89 % selectivity for *N*-phenylhydroxylamine (Table 1, entries 21–22); the lower selectivities obtained with PtNP@PPh_2-PEGPIILS compared with **2** in both solvents results from competing reduction to aniline.

Having identified conditions to obtain *N*-phenylhydroxylamine in high selectivity, the conversion and composition was monitored as a function of time in ethanol at 25 °C to explore the reaction profile. The data in Fig. 3a, obtained by quenching a series of parallel reactions at different times, shows that *N*-phenylhydroxylamine forms cleanly and quantitatively as the nitrobenzene is consumed and that 100 % conversion is reached after only 2 h. The corresponding composition-time profile for the same catalytic reduction carried out in air (Fig. 3b) revealed that the reaction is significantly slower when conducted under air as the conversion only reached 57 % after 2 h and only improved to 69 % after 6 h; interestingly though, only trace amounts of azoxybenzene (2 %) and aniline (4 %) were generated under these conditions and *N*-phenylhydroxylamine was still obtained as major product in 89 % and 91 % selectivity, respectively. The formation of only a minor amount of azoxybenzene is most likely due to mass transfer limited oxidation of the *N*-phenylhydroxylamine as the reaction was conducted in an open Schlenk flask with steady stirring. This was confirmed by exposing a chloroform solution of freshly prepared *N*-phenylhydroxylamine to air as oxidation to azoxybenzene required 360 h to reach completion (Fig. 3c); this oxidation was markedly more facile when the sample was exposed to oxygen. The data in Fig. 3a-c suggest that the high selectivity for *N*-phenylhydroxylamine is due to a combination of the mild conditions and the use of an inert atmosphere as the formation of *N*-phenylhydroxylamine is irreversible under these conditions. To this end, Liu has reported that treatment of *p*-hydroxyaminotoluene with hydrazine in the absence of catalyst results in the formation of a minor amount of *p,p'*-azoxytoluene, presumably due to reversible formation of the nitroso compound arising from incomplete exclusion of air [127].

The heterogeneous nature of **2** was investigated by performing a conventional hot filtration experiment in which two reactions were run in parallel at 25 °C using 0.1 mol% **2** and three mole equivalents of hydrazine hydrate to catalyse the reduction of nitrobenzene. When the conversion reached *ca.* 40 % (time = 30 m in) one of the reaction mixtures was filtered through a 45-μm syringe filter and the composition monitored as a function of time for a further 90 min. The resulting composition-time profile for the pair of parallel reactions (Fig. 4) clearly shows that there is no further conversion after filtration indicating that the active species has been removed *i.e.*, the catalyst is either heterogeneous or leaching of ruthenium generates a much less active or inactive species. This study was supported by a second hot filtration experiment in which a reduction was allowed to reach complete conversion (2 h) after which the reaction mixture was filtered through a 45-μm syringe filter and a fresh portion of nitrobenzene

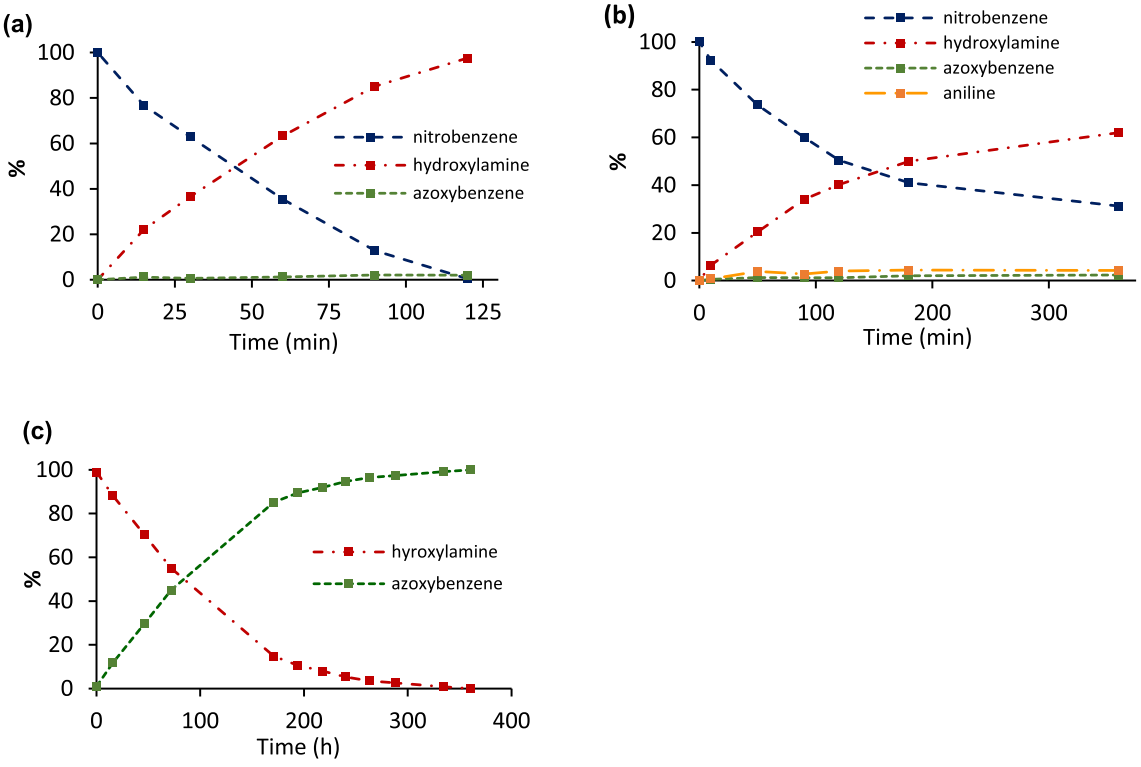

Fig. 3. (a) Composition-time profile for the partial reduction of nitrobenzene conducted under nitrogen in ethanol at 25 °C with 3 mol equivalents of hydrazine hydrate and catalysed by 0.1 mol% **2**. (b) Composition-time profile for the reduction of nitrobenzene conducted under air in ethanol at 25 °C with 3 mol equivalents of hydrazine hydrate and catalysed by 0.1 mol% **2**; (c) Composition-time profile for the oxidation of *N*-phenylhydroxylamine to azoxybenzene in chloroform at 25 °C.

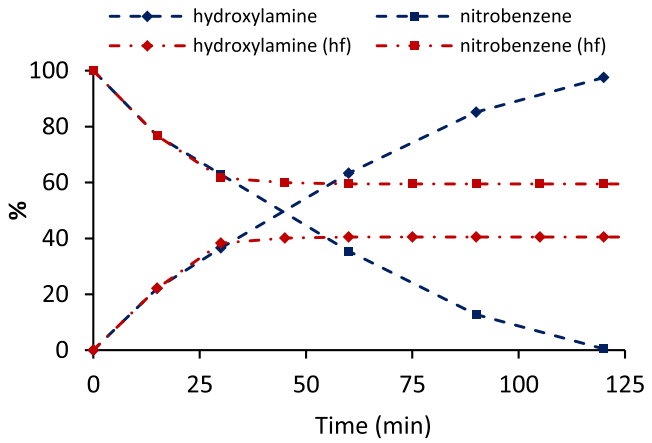

Fig. 4. Hot filtration experiment for the hydrazine hydrate-mediated reduction of nitrobenzene catalysed by 0.1 mol% **2** showing that the reduction is completely quenched after filtration. Blue line – composition of nitrobenzene and *N*-phenylhydroxylamine in the presence of **2**; red lines – composition of nitrobenzene and *N*-phenylhydroxylamine in the presence of **2** with filtration at t = 30 min. (For interpretation of the references to colour in this figure legend, the reader is referred to the web version of this article.)

added to the filtrate and the reaction monitored. The resulting composition-time profile showed no further conversion of nitrobenzene even after stirring for an additional 2 h, which further confirms that the active species has been removed.

The stability and lifetime of **2** as a catalyst for the hydrazine hydrate-mediated reduction of nitrobenzene was investigated by monitoring the activity and selectivity profile during reuse to establish its suitability for scale-up in a continuous flow process as previously reported for the $NaBH_4$ mediated reduction of nitrobenzene using $PdNP@PPh_2$-PEGPIILS as the catalyst [100]. However, the practical difficulties associated with filtering and recovering a small quantity of catalyst after each run meant that it would not be practical to conduct a conventional recycle study. Thus, the activity and selectivity profile for the reduction of nitrobenzene in ethanol was monitored as a function of time for 60 min after which an additional portion of substrate and hydrazine hydrate was added to the flask and the composition monitored for a further 60 min; this protocol was repeated across five reuses to map the catalyst efficacy against reaction time and reuse number. The data in Fig. 5 is encouraging as the catalyst retains good activity in each run; the minor increase in conversion after the first run may be due to reduction of surface ruthenium oxide increasing the number of active metallic ruthenium sites or a morphological change. The gradual reduction in selectivity after the second run is paralleled by the formation of increasing amounts of aniline, which is most likely due to a build-up of hydrazine hydrate as an additional three equivalents is added to the reaction flask after each run; as shown above from a study of the influence on the product distribution of the nitrobenzene:hydrazine mole ratio the use of a large excess of reducing agent results in complete reduction to aniline, even under mild conditions.

Having identified optimum conditions for the selective partial reduction of nitrobenzene to *N*-phenylhydroxylamine under mild conditions, the protocol was applied to the reduction of a range of substituted nitroarenes to explore the efficiency and scope of **2** and to compare its performance against existing systems. Reactions were first conducted under the optimum conditions for the same time (2 h) to obtain comparative performance data as a function of the substrate; if required, reaction times were subsequently adjusted to determine the selectivity at high conversion, full details of which are presented in Table 2. Good conversions were obtained with nitroarenes substituted at the 4-position with electron withdrawing groups such as chloro- and fluoro-, which were both reduced to the corresponding *N*-arylhydroxylamine in high selectivity with no evidence for competing hydrodehalogenation to either nitrobenzene or aniline under these conditions (Table 2, entries 1–3). The reduction of nitroarenes bearing reducible functional groups such as cyano, amido, vinyl and acetyl all occurred with complete chemoselectivity for the nitro group. For example, high yields and selectivities were obtained for the reduction of 4-nitrobenzonitrile and 4-nitrostyrene which reached 98 % and 100 % conversion, respectively, to afford 4-(hydroxyamino) benzonitrile and *N*-(4-vinylphenyl)hydroxylamine in 95 % and 100 % selectivity, respectively, although 4-nitrostyrene required a significantly longer reaction time to achieve a high conversion (Table 2, entries 4–5). Similarly, under the same conditions, 4-nitrobenzamide was reduced to 4-(hydroxyamino)benzamide in 93 % selectivity at 96 % conversion after only 210 min (Table 2, entry 6). While the reduction of 4-nitroacetophenone also occurred with complete chemoselectivity for the nitro group, the selectivity decreased at high conversion due to complete reduction to 4-aminoacetophenone such that the corresponding *N*-arylhydroxylamine was obtained with 76 % selectivity at 100 % conversion after 150 min, with no evidence for the corresponding hydrazone or reduction of the carbonyl (Table 2, entry 7). The reduction of 1,4-dinitrobenzene occurred with complete chemose-

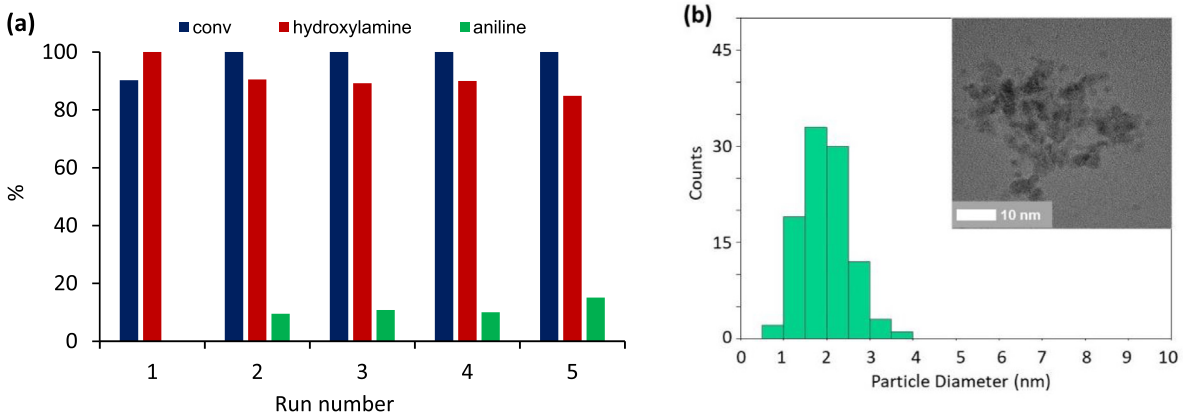

Fig. 5. (a) Recycle study for the selective partial reduction of nitrobenzene conducted at 40 °C in ethanol and catalysed by 0.1 mol% **2** and (b) sizing histogram of RuNPs for **2** after five reuses and a TEM image of the recovered material, revealing an average NP diameter of 1.98 ± 0.56 nm, white scale bar = 10 nm.

Table 2
Partial reduction of aromatic and heteroaromatic nitro compounds to the corresponding hydroxylamine or amine catalysed by 0.1 mol% **2**.[a]

Entry	Substrate	Product	Time (min) [b]	Conv. (%) [b,c]	Selectivity (%) [c,d]
1	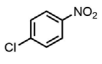	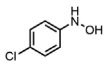	120/180	73/98	95/94
2		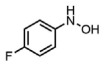	120/180	90/95	87/88
3	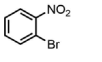		120/180	76/95	100/100
4	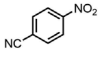	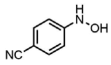	120/90	100/98	84/91
5	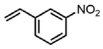	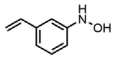	120/480	46/100	100/100
6	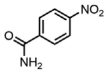	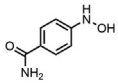	120/210	82/96	94/93
7	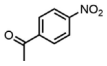	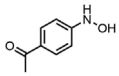	120/150	83/100	90/76
8	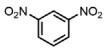	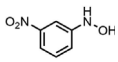	120	97	>99
9	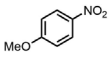	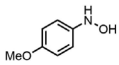	120/360	58/95	90, 88
10	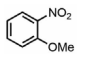		120/330	50/97	98/94
11	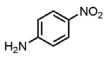	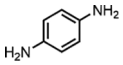	120/1080	6/14	100[e]/100 [e]
12	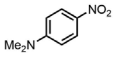	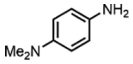	120/4320	7/24	100[e]/100 [e]
13	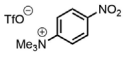	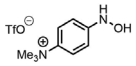	120/4320	23/100	69/71
14			120/1080	31/100	100/93
15			120/150	79/95	92/95
16	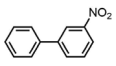	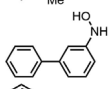	120/180	71/100	100/88
17			120/240	69/95	95/94
18			120/180	66/100	89/86
19	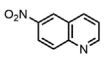	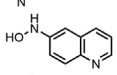	120/240	69/100	100/100
20	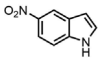	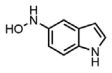	120/1440	12/24	100[e]/100[e]

[a] Reaction conditions: Conducted under nitrogen, 1 mmol substrate, 0.1 mol% **2**, 2 mL ethanol, 3 mmol hydrazine hydrate, 25 °C, time. [b] % Conversion determined by ^{1}H NMR spectroscopy using dioxane as the internal standard. Average of three runs. [c] Reactions were initially run for 120 min to obtain comparative conversion data for each substrate and where required a second reaction was conducted for an appropriate time to reach high conversion; the corresponding reaction times, conversions and selectivities are separated by the / symbol. [d] Selectivity for the hydroxylamine = [% hydroxylamine / (% hydroxylamine + % azoxyarene + % azoarene + % aniline)] × 100%. [e] Selectivity for the corresponding aryl amine.

lectivity for one nitro group to afford the corresponding *N*-4-nitrophenylhydroxylamine with > 99 % selectivity at 96 % conversion, consistent with a previous report for this substrate [46] (Table 2, entry 8). Nitroarenes bearing electron donating groups required longer reaction times, for example, the reduction of 4-nitroanisole required 360 min to reach 96 % conversion with 88 % selectivity for *N*-(4-methoxyphenyl)hydroxylamine while the sterically more demanding 2-nitroanisole reached 96 % conversion with 94 % selectivity for *N*-(2-methoxyphenyl)hydroxylamine after 330 min (Table 2, entries 9–10). The reduction of 4-nitroaniline was also extremely sluggish and only reached 14 % conversion after 18 h, moreover, the fully reduced aniline was obtained as the sole product and there was no evidence for the hydroxylamine i.e. reduction of the electron rich *N*-(4-aminophenyl)hydroxylamine must be facile under these conditions (Table 2, entry 11). Similarly, the reduction of *N*,*N*-dimethyl-4-nitroaniline was also slow under the same conditions and resulted in 7 % conversion to the fully reduced *N*[1],

N^1-dimethylbenzene-1,4-diamine after 2 h (Table 2, entry 12) which only increased to 24 % when the reaction time was extended to 72 h. The low reactivity of these electron rich nitroarenes is consistent with a kinetic and computational study on the hydrogenation of *para*-substituted nitrobenzenes to the corresponding anilines catalysed by gold nanoparticles on titania nanotubes which reported that electron donating groups reduce the rate of hydrogenation compared to nitrobenzene, with $-NH_2$ exerting the largest deactivating effect [128]. This deactivation was explained on the basis of the proposed mechanism for the direct route which involves rate limiting hydrogenation of *N*-phenylhydroxylamine [129–131]. While the low reactivity of 4-nitroaniline and *N,N*-dimethyl-4-nitroaniline obtained under our conditions is consistent with this report, the reduction of their derived *N*-arylhydroxylamines does not appear to be rate limiting as they are both readily reduced to the corresponding amine with no evidence for the hydroxylamine. In this regard, full reduction of electron rich nitroarenes such as phenols, anilines and anisoles has previously been reported with a polystyrene supported RuNP catalyst that is highly selective for the hydrazine hydrate-mediated partial reduction of a range of substituted nitroarenes to the corresponding *N*-aryl and *N*-heteroaryl hydroxylamine [44]. Conversely though, partial reduction of 4-nitroaniline to *N*-(4-aminophenyl) hydroxylamine has been achieved with solid supported PtNPs, albeit with a catalyst loading of 2 mol% [45]. At this stage, we speculate that the complete reduction of 4-amino-substituted nitroarenes to the corresponding arylamine may be facilitated by the electron donating amino group assisting a pathway that involves elimination of OH^- from the hydroxylamine to generate a highly reactive and reducible quinondiimine-derived iminium intermediate that reacts rapidly with a surface hydride to liberate the amine, as shown in Scheme 2. Thus, for electron rich nitroarenes formation of the hydroxylamine appears to be rate limiting under our conditions in ethanol, which is eminently reasonable as it involves transfer of a surface hydride to the nitrogen atom of a nitroarene coordinated to the surface of the nanoparticle and activated by electrostatic interactions with the surface of the polymer (Scheme 2). Decomposition of the hydrazine hydrate to the active Ru-H species and N_2 may well be facilitated by weakening of the N–H bonds through hydrogen bonding between the phosphine oxide on the polymer and a surface coordinated hydrazine, as shown in Scheme 3.

The reduction of the corresponding quaternary ammonium salt, *N,N,N*-trimethyl-4-nitro-anilinium triflate, was investigated to explore whether the electron donating amine was responsible for the low reactivity on the basis that the quaternization would not only quench the electron donor capacity of the amine but would be expected to activate the nitroarene towards reduction. In contrast to *N,N*-dimethyl-4-nitroaniline (Table 2, entry 12), reduction of its trimethylammonium triflate counterpart reached 100 % conversion after 72 h with 71 % selectivity for the corresponding hydroxylamine (Table 2, entry 13); under these conditions the arylamine was identified as the other major species (19 %) together with trace amounts of the azoxyarene (7 %) and the hydrazoarene (3 %), details of which are presented in Figure S2 of the support information. For comparison *N,N*-dimethyl-4-nitroaniline only reached 24 % conversion with 100 % selectivity for the fully reduced N^1,N^1-dimethylbenzene-1,4-diamine in the same time, suggesting that the low reactivity of this substrate may be due to the conjugative electron donating power of the amino group. Although the reduction of *N,N,N*-trimethyl-4-nitro-anilinium triflate is clearly more facile than *N,N*-dimethyl-4-nitroaniline, a significantly longer reaction time was required to reach complete conversion compared to the more conventional electron poor nitroarenes shown in Table 1. To this end, the influence of the triflate anion on catalyst efficacy was investigated by conducting a reduction of nitrobenzene at 25 °C with 0.1 mol% **2** in the presence of 1 mmol of sodium triflate. Under these conditions, the conversion of 14 % (with 100 % selectivity for *N*-phenylhydroxylamine) is significantly lower than that obtained for the same reaction in the absence of salt which reached completion at the same time. Thus, the low reactivity of *N,N,N*-trimethyl-4-nitro-anilinium triflate may be attributed to the anion either saturating the surface active sites on the NP and/or disrupting key hydrogen bonding interactions involved in the decomposition of the hydrazine hydrate. However, as a large excess of nitrogen donor based nitroarene may either saturate the active surface ruthenium sites and deactivate/inhibit the catalyst or modify the course of the reaction, an exploratory study was conducted by pre-treating **2** with *N,N*-dimethyl-4-nitroaniline across a range of pre-stirring times to assess the effect of the potential nitrogen donor group on its activity for the hydrazine hydrate-mediated reduction of nitrobenzene. The resulting conversion against pre-stirring time profile in Fig. S3a reveals that the conversion dropped from 99 % in the absence of *N,N*-dimethyl-4-nitroaniline to 38 % after pre-stirring the catalyst with 1 mmol of *N,N*-dimethyl-4-nitroaniline for 20 min prior to the addition of nitrobenzene *i.e.* a 62 % reduction in activity. Moreover, the passivation appears to be instantaneous as the conversion dropped to 40 % upon direct addition of *N,N*-dimethyl-4-nitroaniline with no pre-stirring. In addition, the conversion continued to drop slightly to 34 % and 29 % when the pre-stirring time was increased to 40 min and 60 min, respectively. Reassuringly, a similar conversion-pre-stirring time profile was obtained for the hydrazine hydrate-mediated reduction of nitrobenzene when the catalyst was pre-stirred with *N,N*-dimethylaniline (Fig. S3b).

The sterically demanding substrate, 1-nitronaphthalene proved to be much more challenging and only reached 31 % conversion with 100 % selectivity for *N*-(naphthalen-1-yl)hydroxylamine after 120 min, however, this improved to 93 % conversion after extending the reaction time to 18 h (Table 2, entry 14). The reduction of other substituted nitroarenes including 2-nitrotoluene and 3-nitrobiphenyl occurred with high selectivity and good conversion to the corresponding *N*-arylhydroxylamine in relatively short reaction times (Table 2, entries 15–16). The same protocol was also effective for the selective reduction of heteroaromatic nitro compounds including 2- and 3-nitropyridine which gave high yields of the corresponding *N*-(pyridinyl)hydroxylamine in relatively short reaction times while 6-nitroquinoline was reduced to *N*-(quinolin-6-yl)hydroxylamine with 97 % selectivity at complete conversion (Table 2, entries 17–19). However, under the same conditions the reduction of 5-nitroindole was slow and only reached 23 % conversion to the fully reduced 5-aminoindole after 24 h which increased to 63 % after 144 h (Table 2, entry 20); this switch in selectivity is perhaps not surprising as the substrate is electron rich (see above). A competition reaction conducted on the reduction of nitrobenzene in the presence of 1 mmol 5-nitroindole and catalysed by 0.1 mol% **2** gave 35 % conversion with 95 % selectivity

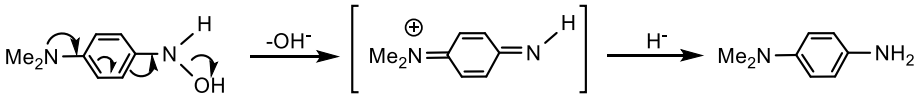

Scheme 2. Proposed pathway for complete reduction of electron rich nitroarenes to the corresponding amine via elimination of OH^- from the hydroxylamine to generate a reducible quinondiimine-derived iminium intermediate that reacts rapidly with a surface hydride to liberate the amine.

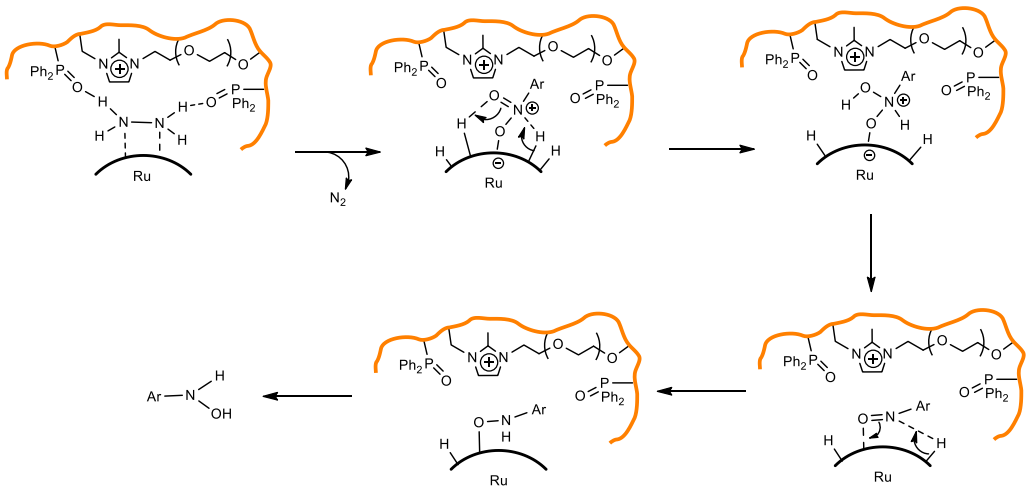

Scheme 3. Possible pathway for the hydrogen bond activated decomposition of hydrazine hydrate and reduction of nitroarenes to their corresponding *N*-arylhydroxylamine.

for *N*-phenylhydroxylamine after 2 h; this is significantly lower than the conversion of 99 % obtained at the same time for the corresponding reaction in the absence of 5-nitroindole and represents a 65 % drop in the activity (Fig. S3c). This reduction in conversion maps closely to that noted above for the pre-treatment of **2** with either *N,N*-dimethyl-4-nitroaniline or *N,N*-dimethylaniline and is consistent with the coordination of the heteroatom donor to the surface of the nanoparticle passivating the active sites. While these competition experiments clearly indicate that heteroatom donors have a marked influence on the efficiency of **2** as a catalyst for the reduction of nitroarenes, we are not sure whether this passivation is due to coordination of the donor atom to the surface of the nanoparticle modifying its reactivity or saturation of the active sites preventing substrate binding; as such, further surface spectroscopic studies will be required to distinguish between these processes.

2.3. Complete reduction of nitroarenes to the arylamine

As there are a host of transition metal nanoparticle-based systems that catalyse the reduction of nitroarenes and heteroaromatic nitro compounds with complete reduction to the corresponding amine, a study was undertaken to identify the conditions required to achieve complete reduction of nitrobenzene with catalyst **2** to compare its efficacy against existing catalysts. Using the conditions described above as a lead, the reduction of nitrobenzene was monitored as a function of time in ethanol at 40 °C using a 0.1 mol% loading of **2**. The resulting composition-time profile in Fig. 6a shows that the nitrobenzene is completely consumed after only 45 min during which time *N*-phenylhydoxylamine is formed as the sole product; the minor amount of azoxybenzene is generated during exposure of the reaction mixture to air during the aqueous work-up as described above. Longer reaction times resulted in gradual consumption of the *N*-phenylhydroxylamine to afford aniline which was obtained in quantitative yield after 16 h, however, complete conversion could be obtained in a much shorter reaction time by increasing the temperature to 60 °C. Reassuringly, a reduction of nitrobenzene conducted in d_6-ethanol at 40 °C using 0.1 mol % **2** and three equivalents of hydrazine hydrate showed a similar composition profile (Fig. 6b), albeit over a much longer timescale as the reaction was monitored in a sealed NMR tube to prevent exposure to air; the absence of azoxybenzene in this sample confirms that the reduction occurs via the direct pathway and that azoxybenzene is generated by serendipitous exposure to air. The lower selectivity for *N*-phenylhydroxylamine obtained when the reduction was conducted in an NMR tube compared with a flask is most likely due to the longer reaction time due to the lack of stirring or agitation. This protocol was applied to representative examples of electron rich and electron poor substates and complete conversion of 1-chloro-4-nitrobenzene, 5-nitroindole, *N,N*-

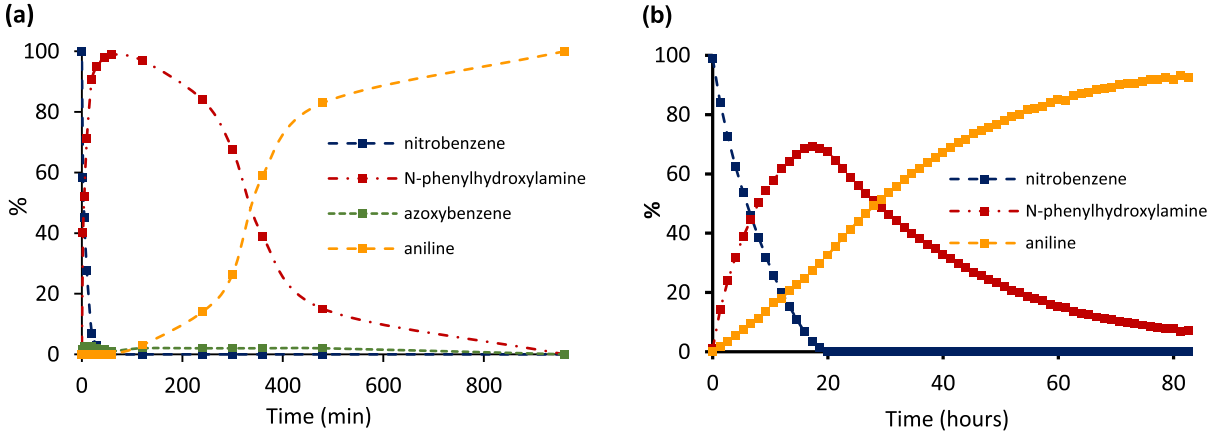

Fig. 6. Composition profile as a function of time for the hydrazine hydrate-mediated reduction of nitrobenzene at 40 °C catalysed by 0.1 mol% **2** consistent with direct reduction to aniline via *N*-phenylhydroxylamine. (a) Data obtained by sampling a reaction conducted in ethanol and (b) reaction conducted in d_6-ethanol and data obtained by monitoring the reaction in a sealed NMR tube.

dimethylamine-4-nitrobenzene-4-nitroanisole and 4-nitroanisole to 1-chloroaniline, 5-aminoindole, N^1,N^1-dimethylbenzene-1,4-diamine and 4-aminoanisole, respectively, was obtained after 5 h by conducting the reduction at 60 °C. A comparison with the recent literature reveals that **2** competes with existing systems as the TOF of 200 h^{-1} obtained in ethanol at 60 °C is markedly higher than the 57 h^{-1} for a diruthenium catalyst in ethanol at 80 °C [127], a significant improvement on 10 h^{-1} for polymethylhydrosiloxane derived PdNP [132], 20 h^{-1} for carbon nitride supported palladium nanoparticles [122] and 60 h^{-1} for solid supported PdNPs [133] but lower than that of 1140 h^{-1} for RuNPs immobilised on porous organic polymers [121] and 800 h^{-1} for PdNPs immobilised on carbon nanospheres [123].

3. Conclusions

This study has revealed that ruthenium nanoparticles stabilised by a phosphine oxide decorated polymer immobilised ionic liquid (RuNP@O = PPh_2-PEGPIILS) is a remarkably efficient and selective catalyst for the partial reduction of nitrobenzene to the corresponding *N*-phenylhydoxylamine. The efficacy and selectivity of the catalyst depends on both the solvent and the reducing agent and reactions conducted at room temperature under nitrogen in ethanol using hydrazine hydrate as the reducing agent gave the highest selectivity (>99 %). The initial TOF of 8,760 h^{-1} obtained at 40 °C with a catalyst loading of 0.1 mol% is among the highest to be reported for a ruthenium nanoparticle catalysed reduction of nitrobenzene to *N*-phenylhydroxylamine and is a significant improvement on commercial 5 wt/% Ru/C which gave a low conversion to a mixture of *N*-phenylhydroxylamine and aniline. This system compliments its AuNP counterpart which catalyses the sodium borohydride mediated reduction of nitrobenzene to afford azoxybenzene as the sole product in ethanol and *N*-phenylhydroxylamine with > 99 % selectivity in water. A wide range of substituted aromatic and heteroaromatic nitroarenes were reduced to the corresponding *N*-arylhydroxylamine in high yields and with excellent selectivity, with the exception of 4-amino-substituted nitroarenes which resulted in complete reduction to the corresponding aniline. Complete reduction of the 4-amino substituted nitroarenes was attributed to the electron donating amino group facilitating elimination of OH^- to generate a highly reactive and reducible quinondiimine-derived iminium intermediate that reacts rapidly with a surface hydride to liberate the amine. A reusability study on the selective reduction of nitrobenzene to *N*-phenylhydroxylamine showed that **2** was robust as it could be recycled five times with negligible change in activity and only a slight decrease in selectivity. The modular construction of the PIIL supports will enable the composition to be modified to explore which components are necessary to achieve the highest selectivity and to examine how the ionic microenvironment and density, the number and type of heteroatom donor and the hydrophilicity and porosity influences selectivity. To this end, catalyst modifications and in operando surface investigations and kinetic studies are currently underway to develop a more detailed understanding of this system.

4. Experimental

4.1. General comments

4.1.1. Synthesis of RuNP@O = PPh_2-PEGPIILS (**2**)

A round bottom flask was charged with **1** (4.00 g, 2.68 mmol) and ethanol (55 mL). To this, a solution of $RuCl_3{\cdot}3H_2O$ (0.56 g, 2.68 mmol) in ethanol (20 mL) was added in a single portion and the resulting mixture stirred vigorously for 5 h at room temperature. After this time, an aqueous solution of $NaBH_4$ (0.81 g, 21.44 mmol in 10 mL of water) was added dropwise and the suspension stirred for an additional 18 h at room temperature before concentrating to near dryness under vacuo. The crude black solid was triturated with cold acetone (2 × 100 mL), washed with water (100 mL) and ethanol (2 × 40 mL) and the resulting black solid was recovered from the washings via centrifugation followed by filtration through a frit. The final product was washed with ether until a fine black powder was obtained. The powder was then dried in *vacuo* to afford the product in 78 % yield (3.32 g). ICP-OES data: 1.83 wt% ruthenium and a ruthenium loading of 0.18 mmol·g^{-1}.

4.2. General procedure for reduction of nitroarenes to arylhydroxylamines

Under an inert atmosphere, an oven-dried Schlenk flask was charged with **2** (5.6 mg, 0.1 mol%), hydrazine monohydrate (0.15 mL, 3.0 mmol) and anhydrous ethanol (2 mL). After allowing the resulting suspension to stir for 5 min, nitroarene (1.0 mmol) was added and the mixture stirred at 25 °C for the allocated time. The reaction mixture was quenched by addition of deionized water (5 mL), the product extracted with ethyl acetate (3 × 5 mL), the organic fractions collected, and the solvent removed under reduced pressure to obtain the product. The residue was analyzed by ^{1}H NMR spectroscopy using 1,4-dioxane as internal standard to quantify the composition of starting material and products and determine the selectivity.

4.3. General procedure for reduction of nitroarenes to arylamines

Under an inert atmosphere, an oven-dried Schlenk flask was charged with **2** (5.6 mg, 0.1 mol%), hydrazine monohydrate (0.15 mL, 3.0 mmol) and anhydrous ethanol (2 mL). After allowing the resulting suspension to stir for 5 min, nitroarene (1.0 mmol) was added and the mixture stirred at 60 °C for the appropriate time. The reaction mixture was diluted with deionized water (5 mL), the product extracted with ethyl acetate (3 × 5 mL), the organic fractions collected, and the solvent removed under reduced pressure to yield the product. The residue was analyzed by ^{1}H NMR spectroscopy using 1,4-dioxane as internal standard to quantify the composition of starting material and products and determine the selectivity.

4.4. Procedure for the hot filtration study

Nitrobenzene (0.103 mL, 1.0 mmol) was reduced to *N*-phenylhydroxylamine at 25 °C following the general procedure described above. After 30 min the reaction mixture was filtered through a 0.45-μm syringe filter into a clean Schlenk flask under an inert atmosphere. The filtered reaction mixture was then stirred at 25 °C for a further 90 min and the progress of the reaction monitored as a function of time by removing aliquots every 15 min for analysis by NMR spectroscopy.

4.5. Procedure for the catalyst reuse study

Nitrobenzene (0.102 mL, 1.0 mmol) was reduced to *N*-phenylhydroxylamine a 40 °C following the general protocol above, monitoring the progress of the reaction by ^{1}H NMR spectroscopy. After 1 h, the reaction flask was recharged with a further portion of nitrobenzene and an additional three equivalents of hydrazine hydrate (0.150 mL, 3.0 mmol) and the procedure repeated. Following the 5th run the catalyst was isolated, washed with water (2 × 10 mL) and ethyl acetate (2 × 10 mL) and analysed by TEM.

4.6. General procedure for the poisoning the studies as a function of Pre-stirring time

An oven-dried Schlenk flask cooled to room temperature under vacuum, back-filled with nitrogen and charged with **2** (5.6 mg, 0.1 mol%), hydrazine monohydrate (0.15 mL, 3 mmol), anhydrous ethanol (2 mL) and *N,N*-dimethyl-4-nitroaniline, *N,N*-dimethylaniline or 5-nitroindole (1.0 mmol) and the resulting mixture was stirred for the allocated time (0, 20, 40 or 60 min) to explore the effect of pre-stirring time on catalyst efficacy. Reaction was initiated by the addition of nitrobenzene (0.103 mL, 1.0 mmol) and the mixture was left to stir for 2 h at room temperature. The reaction mixture was quenched by addition of deionized water (5 mL), the product extracted with ethyl acetate (3 × 5 mL), the organic fractions collected, and the solvent removed under reduced pressure. The resulting residue was analyzed by ^{1}H NMR spectroscopy using 1,4-dioxane as internal standard (1.0 mmol) to quantify the composition of starting material and products and determine the selectivity.

Data availability

Data will be made available on request.

Declaration of Competing Interest

The authors declare that they have no known competing financial interests or personal relationships that could have appeared to influence the work reported in this paper.

Acknowledgements

R.P. gratefully acknowledges the Engineering and Physical Sciences Centre for Doctoral Training in Renewable Energy Northeast Universities ('ReNU') EP/S023836/1 for a studentship and H.Y. A. gratefully acknowledges Taibah University, Saudi Arabia for a Scholarship. We also thank Dr Tracey Davey for the SEM images (Faculty of Medical Sciences, Newcastle University) and Zabeada Aslam and the Leeds electron microscopy and spectroscopy centre (LEMAS) at the University of Leeds for TEM analysis. This research was funded through a studentship (Anthony Griffiths) awarded by the Engineering and Physical Sciences Centre for Doctoral Training in Molecules to Product (EP/SO22473/1). The authors greatly acknowledge their support of this work. The Henry Royce Institute (EPSRC grants: EP/P022464/1, EP/R00661X/1), which funded the VXSF Facilities with the Bragg Centre for Materials Research at Leeds. This article is dedicated to the memory of Professor Stephen A. Westcott (Canada Research Chair holder in the Department of Chemistry & Biochemistry, Mount Allison University, Canada) who recently passed away; a fantastic scientist, a great ambassador for chemistry teaching and research in Canada and across the globe, a generous, genuine, and kind human being but most of all the best and most sincere of friends.

Appendix A. Supplementary material

Supplementary data to this article can be found online at https://doi.org/10.1016/j.jcat.2022.11.023.

References

[1] The Chemistry of Hydroxylamines, Oximes and Hydroxamic acids, Rappaport, Z. J. Wiley and Sons Ltd, 2009.
[2] W. Uhl, A. Kyriatsoulis, Namen and Schlagwortreaktionen in der Organischen Chemie, Vieweg+Teubner Verlag, Wiesbaden, 1984.
[3] P.M. Vyas, S. Roychowdhury, P.M. Woster, C.K. Svensson, Reactive oxygen species generation and its role in the differential cytotoxicity of the arylhydroxylamine metabolites of sulfamethoxazole and dapsone in normal human epidermal keratinocytes, Biochem. Pharmacol. 70 (2005) 275–286.
[4] J.S. Yadav, B.V.S. Reddy, P. Streedhar, Three-component one-pot synthesis of α-hydroxylamino phosphonates using ionic liquids, Adv. Synth. Catal. 345 (2003) 564–567.
[5] C.K. Svensson, Do Arylhydroxylamine metabolites mediate idiosyncratic reactions associated with sulfonamides?, Chem Res. Toxicol. 16 (2003) 1035–1043.
[6] D.K. Nio, K. Zhao, Concerted conjugate addition of nucleophiles to alkenoates. Part I: mechanism of N-alkylhydroxylamine additions, J. Am. Chem. Soc. 121 (1999) 2456–2459.
[7] M.G. Kallitsakis, D.I. Ioannou, M.A. Terzidis Michael A. Terzidis, G.E. Kostakis, I.N. Lykakis, Selective photoinduced reduction of nitroarenes to *N*-arylhydroxylamines, Org. Lett. 22 (2020) 4339−4343.
[8] P. Kumar, Pharmacology and Therapeutics for Dentistry, 7th ed.;., Elsevier, 2017, pp. 457–487.
[9] Y. Qu, J.C. Spain, Environ. Microbiol. 13 (2011) 1010–1017.
[10] R. Singh, U. Manjunatha, H.I. Boshoff, Y.H. Ha, P. Niyomrattanakit, R. Ledwidge, C.S. Dowd, I.Y. Lee, P. Kim, L. Zhang, S. Kang, T.H. Keller, J. Jiricek, C.W. Barry, 3rd Science 2008, 322, 1392−1395.
[11] M.D. Corbett, B.R. Chipko, Synthesis and Antibiotic properties of chloramphenicol reduction products, agents, and chemotherapy 13 (1978) 193–198.
[12] K. Shudo, T. Okamoto, Carcinogenic reactions. Arylamination with arylhydroxylamines, Tet. Lett. 21 (1973) 1839–1842.
[13] K. Shudo, T. Ohta, T. Okamoto, Acid-catalyzed reactions of *N*-arylhydroxylamines and related compounds with benzene. Iminium-benzenium ions.
[14] H. Takeuchi, J-i. Tateiwa, S. Hata, K. Tsutsumi, Y. Osaki, Selective Aromatic N-Substitution with *N*-(4-t)hydroxylamine by addition of polar aprotic or diethereal solvent, Eur. J. Org. Chem. (2003) 3920–3922.
[15] A.D. McGill, W. Zhang, J. Wittbrodt, J. Wang, H.B. Schlegel, P.G. Wang, para-Substituted N-nitroso-N-oxybenzenamine ammonium salts: a new class of redox-sensitive nitric oxide releasing compounds, Biorg, Med. Chem. 8 (2000) 405–412.
[16] A.T. Balaban, R.E. Garfield, M.J. Lesko, W.A. Seitz, Synthesis, and spectral data of some new *N*-nitroso-*N*-phenylhydroxylamine (cupferron) derivatives, Org. Prep. Proced. Int. 30 (1998) 439–446.
[17] J.D. Spence, A.E. Raymond, D.E. Norton Condensations of *N*-arylhydroxylamines for the preparation of 5,5′-di-tert-butyl-2,2′-dihydroxydiphenylamine, Tet. Lett. 44 (2003) 849-851.
[18] F. Ahmad, J.B. Hughes, Reactivity of partially reduced arylhydroxylamine and nitrosoarene metabolites of 2,4,6-trinitrotoluene (TNT) toward biomass and humic acids, Environ. Sci. Technol. 36 (2002) 4370–4381.
[19] C.-M. Ho, T.-C. Lau, Copper-catalyzed amination of alkenes and ketones by phenylhydroxylamine, New J. Chem. 24 (2000) 859–863.
[20] R.S. Srivastava, K.M. Nicholas, On the mechanism of allylic amination catalyzed by iron salts, J. Am. Chem. Soc. 119 (1997) 3302–3310.
[21] R.N. Ram, V.K. Soni, Synthesis of 3-alkylbenzoxazolones from N-alkyl-N-arylhydroxylamines by contiguous O-trichloroacetylation, trichloroacetoxy ortho-shift, and cyclization sequence, J. Org. Chem. 78 (2013) 11935–11947.
[22] E. Bamberger, Ber. Dtch. Chem. Ges. Chem. 27 (1894) 1548–1557.
[23] Y.A. Wang, L.W. Ye, L.M. Zhang, Au-catalyzed synthesis of 2-alkylindoles from N-arylhydroxylamines and terminal alkynes, Chem. Commun. 47 (2011) 7815–7817.
[24] R.B. Harris, I.B. Wilson, Synthesis of tert-butyl aminocarbonate, a new type of compound that can be used to acylate amines, Tett. Lett. 24 (1983) 231–232.
[25] C. Kashima, N. Yoshiwara, Y. Omote, Alkylation of aminohydroxy anion, dissociated species of hydroxylamine, Tett. Lett. 23 (1982) 2955–2956.
[26] L.A. Carpino, C.A. Giza, B.A. Carpino, O-Acylhydroxylamines. I. Synthesis of O-benzoylhydroxylamine, J. Am. Chem. Soc. 81 (1959) 955–957.
[27] D. Beaudoin, J.D. Wuest, Synthesis of *N*-arylhydroxylamines by Pd-catalyzed coupling, Tet. Lett. 52 (2011) 2221–2223.
[28] H. Feuer, B.F. Vincent Jr., R.S. Bartlett, The Reduction of Oximes with Diborane. A New Synthesis of N-Monosubstituted Hydroxylamines, J. Org. Chem. 30 (1965) 2877–2880.
[29] H. Feuer, R.S. Bartlett, B.F. Vincent Jr., R.S. Anderson, Diborane reduction of nitro salts. A new synthesis of *N*-monosubstituted hydroxylamines, J. Org. Chem. 30 (1965) 2880–2882.
[30] P.D. Ren, X.W. Pan, Q.H. Jin, Z.P. Yao, Reduction of nitroarenes to *N*-arylhydroxylamines with $KBH_4/BiCl_3$ system, Synth. Commun. 27 (1997) 3497–3503.
[31] K. Yanada, H. Yamaguchi, H. Meguri, S. Uchida, Selenium-catalysed reduction of aromatic nitro compounds to *N*-arylhydroxylamines, J. C. S, Chem. Commun. (1986) 1655–1656.
[32] M.S. Mourad, R.S. Varma, G.W. Kabalka, Reduction of α,β -unsaturated nitro compounds with boron hydrides: A new route to *N*-substituted hydroxylamines, J. Org. Chem. 50 (1985) 133–135.
[33] H. Feuer, B.F. Vincent, A convenient synthesis of *N*-alkylhydroxylamines, J. Am. Chem. Soc. 84 (1962) 3771–3772.
[34] A.D. McGill, W. Zhang, J. Wittbrodt, J. Wang, H.B. Schlegel, P.G. Wang, para-substituted *N*-nitroso-*N*-oxybenzenamine ammonium salts: a new class of redox-sensitive nitric oxide releasing compounds, Bioorg. Med. Chem. 8 (2000) 405–412.
[35] P. Ren, T. Dong, S. Wu, Synthesis of *N*-arylhydroxylamines by antimony-catalyzed reduction of nitroarenes, Synth. Commun. 27 (1997) 1547–1552.

[36] S.Q. Xun, L.R. Wen, J. Kun, Z.Z. Xi, Z. De Feng, Ultrasound-promoted highly chemoselective reduction of aromatic nitro compounds to the corresponding N-arylhydroxylamines using zinc and $HCOONH_4$ in CH_3CN, Chem. Lett. 35 (2006) 226–227.
[37] S. Ung, A. Falguières, A. Guy, C. Ferroud, Ultrasonically activated reduction of substituted nitrobenzenes to corresponding *N*-arylhydroxylamines, Tet. Lett. 46 (2005) 5913–5917.
[38] M. Bartra, P. Romea, F. Urpí, J. Vilarrasa, A fast procedure for the reduction of azides and nitro compounds based on the reducing ability of $Sn(SR)_3$-species, Tetrahedron 46 (1990) 587–594.
[39] S. Liu, Y. Wang, J. Jiang, Z. Jin, The selective reduction of nitroarenes to N-arylhydroxylamines using Zn in a CO_2/H_2O system, Green Chem. 11 (2009) 1397–1400.
[40] I.D. Entwistle, T. Gilkerson, R.A.W. Johnstone, R.P. Telford, Rapid catalytic transfer reduction of aromatic nitro compounds to hydroxylamines, Tetrahedron 34 (1978) 213–215.
[41] P.W. Oxley, B.M. Adger, M.J. Sasse, M.A. Forth, *N*-Acetyl-*N*-phenylhydroxylamine via catalytic transfer hydrogenation of nitrobenzene using hydrazine and rhodium on carbon, Org. Synth. 67 (1989) 187–192.
[42] L. Pernoud, J.P. Candy, B. Didillon, R. Jacquot, J.M. Basset, Selective hydrogenation of nitrobenzene in phenylhydroxylamine on silica supported platinum catalysts, Stud. Surf. Sci. Catal. 130 (2000) 2057–2062.
[43] D.V. Jawale, E. Gravel, C. Boudet, N. Shah, V. Geertsen, H. Li, I.N.N. Namboothiri, E. Doris, Selective conversion of nitroarenes using a carbon nanotube-ruthenium nanohybrid, Chem. Commun. 51 (2015) 1739–1742.
[44] J.H. Tyler, S.H. Nazari, R.H. Patterson, V. Udumula, S.J. Smith, Synthesis of *N*-aryl and *N*-heteroaryl hydroxylamines via partial reduction of nitroarenes with soluble nanoparticle catalysts, Tetrahedron Lett. 58 (2017) 82–86.
[45] A.K. Shila, P. Das, Solid supported platinum(0) nanoparticles catalyzed chemoselective reduction of nitroarenes to *N*-arylhydroxylamines, Green Chem. 15 (2013) 3421–3428.
[46] E.H. Boymans, P.T. Witte, D. Vogt, A Study on the selective hydrogenation of nitroaromatics to *N*-arylhydroxylamines using a supported Pt nanoparticle catalyst, Catal, Sci. Technol. 5 (2015) 176–183.
[47] D. Bhattacherjee, A. Shaifali, G.V. Kumar, P.D. Zyryanov, Polystyrene stabilized iridium nanoparticles catalyzed chemo- and regio-selective semi-hydrogenation of nitroarenes to *N*-arylhydroxylamines, Mol. Catal. 514 (2021).
[48] Y. Takenaka, T. Kiyosu, J.C. Choi, T. Sakakura, H. Yasuda, Selective synthesis of *N*-aryl hydroxylamines by the hydrogenation of nitroaromatics using supported platinum catalysts, Green Chem. 11 (2009) 1385–1390.
[49] S.L. Karwa, R.A. Rajadhyaksha, Selective catalytic hydrogenation of nitrobenzene to phenylhydroxylamine, Ind. Eng. Chem. Soc. 26 (1987) 1746–1750.
[50] Y. Takenaka, T. Kiyosu, G. Mori, J.-C. Choi, T. Sakakura, H. Yasuda, Selective hydrogenation of nitroalkane to *N*-alkyl hydroxylamine over supported palladium catalysts, Catal. Today 164 (2011) 580–584.
[51] Z. Yan, X. Xie, Q. Song, F. Ma, X. Sui, Z. Huo, M. Ma, Tandem selective reduction of nitroarenes catalyzed by palladium nanoclusters, Green Chem. 22 (2020) 1301–1307.
[52] G. Chen, C. Xu, X. Huang, J. Ye, L. Gu, G. Li, Z. Tang, B. Wu, H. Yang, Z. Zho, Z. Zhou, G. Fu, N. Zheng, Interfacial electronic effects control the reaction selectivity of platinum catalysts, Nature Mat. 15 (2016) 564–569.
[53] D. Li, G. Lu, C. Cai, Modified cellulose with tunable surface hydrophilicity/hydrophobicity as a novel catalyst support for selective reduction of nitrobenzene, Catal. Commun. 137 (2020).
[54] For a comprehensive and highly informative review on the impact of ligands on heterogeneous nanocatalysis see: The critical impacts of ligands on nanocatalysis: A review, L. Lu, Z. Zou, B. Fang, ACS Catal. 11 (2021) 6020–6058.
[55] K. Liu, R. Qin, N. Zheng, Insights into the interfacial effects in heterogeneous metal nanocatalysts toward selective hydrogenation, J. Am. Chem. Soc. 143 (2021) 4483–4499.
[56] For an insightful account on metal nanoparticles immobilised on molecularly modified surfaces for controlled hydrogenation and hydrogenolysis see: A. Bordet and W. Leitner, Metal nanoparticles immobilized on molecularly modified surfaces: versatile catalytic systems for controlled hydrogenation and hydrogenolysis, Acc. Chem. Res. 54 (2021) 2144–2157.
[57] L.M. Rossi, J.L. Fiorio, M.A.S. Garcia, C.P. Ferraz, The role and fate of capping ligands in colloidally prepared metal nanoparticle catalysts, Dalton Trans. 47 (2018) 5889–5915.
[58] S. Campisi, M. Schiavoni, C.E. Chan-Thaw, A. Villa, Untangling the role of the capping agent in nanocatalysis: recent advances and perspectives, Catalysts 6 (2016) 185.
[59] X. Wang, Y.-F. Jiang, Y.-N. Liu, A.-W. Xu, Erbium oxide as a novel support for palladium nanocatalysts with strong metal–support interactions: remarkable catalytic performance in hydrogenation reactions, New J. Chem. 42 (2018) 19901–19907.
[60] M. Sankar, Q. He, R.V. Engel, M.A. Sainna, A.J. Logsdail, A. Roldan, D.J. Willock, N. Agarwal, C.J. Kiely, G.J. Hutchings, Role of the Support in Gold-Containing Nanoparticles as Heterogeneous Catalysts, Chem. Rev. 120 (2020) 3890–3938.
[61] S. Jayakumar, A. Modak, M. Guo, H. Li, X. Hu, Q. Yang, Ultrasmall platinum stabilized on triphenylphosphine-modified silica for chemoselective hydrogenation, Chem. Eur. J. 23 (2017) 7791–7797.
[62] Z. Wang, H. Jiang, Efficient palladium and ruthenium nanocatalysts stabilized by phosphine functionalized ionic liquid for selective hydrogenation, RSC Adv. 5 (2015) 34622–34629.
[63] H. Jiang, X. Zheng, Tuning the chemoselective hydrogenation of aromatic ketones, aromatic aldehydes and quinolines catalyzed by phosphine functionalized ionic liquid stabilized ruthenium nanoparticles, Catal. Sci. Technol. 5 (2015) 3728–3734.
[64] J.L. Castlebou, E. Bresó-Femenia, P. Blondeau, B. Chaudret, S. Castillón, C. Claver, G. Cyril, Tuning the selectivity in the hydrogenation of aromatic ketones catalyzed by similar ruthenium and rhodium nanoparticles, ChemCatChem 6 (2014) 3160–3168.
[65] M. Ibrahim, M.A.S. Garcia, L.L.R. Vono, M. Guerrero, P. Lecante, L.M. Rossi, K. Philippot, Polymer versus phosphine stabilized Rh nanoparticles as components of supported catalysts: implication in the hydrogenation of cyclohexene model molecule, Dalton Trans. 45 (2016) 17782–17791.
[66] Y. Lei, Z. Chen, G. Lan, R. Wang, X.-Y. Zhou, Pd nanoparticles stabilized with phosphine-functionalized porous ionic polymer for efficient catalytic hydrogenation of nitroarenes in water, N. J. Chem. 44 (2020) 3681–3689.
[67] G.D. Kalita, P. Sarmah, P. Kr, L. Saikia, P.D. Saikia, Selective hydrogenation of nitroarenes to amines by ligand-assisted Pd nanoparticles: influence of donor ligands on catalytic activity, N. J. Chem. 43 (2019) 4253–4260.
[68] L. Wu, Z.-W. Li, F. Zhang, Y.-M. He, Q.-H. Fan, Air-Stable and highly active dendritic phosphine oxide-stabilized palladium nanoparticles: preparation, characterization and applications in the carbon-carbon bond formation and hydrogenation reactions, Adv. Synth. Catal. 350 (2008) 846–862.
[69] I. Cano, A.M. Chapman, A. Urakawa, P.W.M.N. van Leeuwen, Air-stable gold nanoparticles ligated by secondary phosphine oxides for the chemoselective hydrogenation of aldehydes: Crucial role of the ligand, J. Am. Chem. Soc. 136 (2014) 2520–2528.
[70] N. Almora-Barrios, I. Cano, P.W.M.N. van Leeuwen, N. Lopez, Concerted chemoselective hydrogenation of acrolein on secondary phosphine oxide decorated gold nanoparticles, ACS Catal. 7 (2017) 3949–3954.
[71] I. Cano, M.A. Huertos, A.M. Chapman, G. Buntkowsky, T. Gutmann, P.B. Groszewicz, P.W.M.N. van Leeuwen, Air-stable gold nanoparticles ligated by secondary phosphine oxides as catalyst for the chemoselective hydrogenation of substituted aldehydes: a remarkable ligand effect, J. Am. Chem. Soc. 137 (2015) 7718–7727.
[72] M. Guo, H. Li, Y. Ren, X. Ren, Q. Yang, Ca Li, Improving catalytic hydrogenation performance of Pd nanoparticles by electronic modulation using phosphine ligands, ACS Catal. 8 (2018) 6476–6485.
[73] X. Ren, M. Guo, H. Li, C. Li, L. Yu, J. Liu, Q. Yang, Microenvironment engineering of ruthenium nanoparticles incorporated into silica nanoreactors for enhanced hydrogenations, Angew. Chem. Int. Ed. 58 (2019) 14483–14488.
[74] S.G. Kwon, G. Krylova, A. Sumer, M.M. Schwartz, E.E. Bunel, C.L. Marshall, S. Chattopadhyay, B. Lee, J. Jellinek, E.V. Shevchenko, Capping Ligands as Selectivity Switchers in Hydrogenation Reactions, Nano Lett. 12 (2012) 5382–5388.
[75] W. Long, N.A. Brunelli, S.A. Didas, E.W. Ping, C.W. Jones, Amino polymer–silica composite-supported Pd catalysts for selective hydrogenation of alkynes, ACS Catal. 3 (2013) 1700–1708.
[76] F.P. da Silva, J.L. Fiorio, L.M. Rossi, Tuning the catalytic activity and selectivity of Pd nanoparticles using ligand-modified supports and surfaces, ACS Omega 2 (2017) 6014–6022.
[77] Z. Guo, C. Xiao, R.V. Maligal-Ganesh, L. Zhou, T.W. Goh, X. Li, D. Tesfagaber, A. Thiel, W. Huang, Pt nanoclusters confined within metal–organic framework cavities for chemoselective cinnamaldehyde hydrogenation, ACS Catal. 4 (2014) 1340–1348.
[78] I. Schrader, J. Warneke, J. Backenköhler, S. Kunz, Functionalization of platinum nanoparticles with l-proline: simultaneous enhancements of catalytic activity and selectivity, J. Am. Chem. Soc. 137 (2015) 905–912.
[79] H. Liu, Q. Mei, S. Li, Y. Yang, Y.Y. Wang, H. Liu, L.R. Zheng, P. An, J. Zhang, B. Han, Selective hydrogenation of unsaturated aldehydes over Pt nanoparticles promoted by the cooperation of steric and electronic effects, Chem. Commun. 54 (2018) 908–911.
[80] M.R. Axet, S. Conejero, I.C. Gerber, Ligand effects on the selective hydrogenation of nitrobenzene to cyclohexylamine using ruthenium nanoparticles as catalysts, ACS Appl. Nano. Mater. 1 (2018) 5885–5894.
[81] M. Guo, C. Li, Q. Yang, Accelerated catalytic activity of Pd NPs supported on amine-rich silica hollow nanospheres for quinoline hydrogenation, Catal. Sci. Technol. 7 (2017) 2221–2227.
[82] B. Wu, H. Huang, J. Yang, N. Zheng, G. Fu, Selective hydrogenation of α, β-unsaturated aldehydes catalyzed by amine-capped platinum-cobalt nanocrystals, Angew. Chem. Int. Ed. 51 (2012) 3440–3443.
[83] S. Rana, S.B. Jonnalagadda, A facile synthesis of Cu–Ni bimetallic nanoparticle supported organo functionalized graphene oxide as a catalyst for selective hydrogenation of p-nitrophenol and cinnamaldehyde, RSC Adv. 7 (2017) 2869–2879.
[84] J.B. Ernst, C. Schwermann, G. Yokota, M. Tada, S. Muratsugu, N.L. Doltsinis, F. Glorius, Molecular adsorbates switch on heterogeneous catalysis: induction of reactivity by N-heterocyclic carbenes, J. Am. Chem. Soc. 139 (2017) 9144–9147.
[85] J.B. Ernst, S. Muratsugu, F. Wang, M. Tada, F. Glorius, Tunable heterogeneous catalysis: N-heterocyclic carbenes aslLigands for supported heterogeneous $Ru/K\text{-}Al_2O_3$ catalysts to tune reactivity and selectivity, J. Am. Chem. Soc. 138 (2016) 10718–10721.

[86] L.M. Martínez-Prieto, A. Ferry, L. Rakers, C. Richter, P. Lecante, K. Philippot, B. Chaudret, F. Glorius, Long-chain NHC-stabilized RuNPs as versatile catalysts for one-pot oxidation/hydrogenation reactions, Chem. Commun. 52 (2016) 4768–4771.
[87] C. Richter, K. Schaepe, F. Glorius, B.J. Ravoo, Tailor-made N-heterocyclic carbenes for nanoparticle stabilization, Chem. Commun. 50 (2014) 3204–3207.
[88] P. Lara, L.M. Martínez-Prieto, M. Roselló-Merino, C. Richter, F. Glorius, S. Conejero, K. Philippot, B. Chaudret, NHC-stabilized Ru nanoparticles: Synthesis and surface studies, Nano-Struct. Nano-Obj. 6 (2016) 39–45.
[89] A. Rühling, K. Schaepe, L. Rakers, B. Vonhören, P. Tegeder, B.J. Ravoo, F. Glorius, Modular bidentate hybrid NHC-thioether ligands for the stabilization of palladium nanoparticles in various solvents, Angew. Chem. Int. Ed. 55 (2016) 5856–5860.
[90] A. Ferry, K. Schaepe, P. Tegeder, C. Richter, K.M. Chepiga, B.J. Ravoo, F. Glorius, Negatively charged N-heterocyclic carbene-stabilized Pd and Au nanoparticles and efficient catalysis in water, ACS Catal. 5 (2015) 5414–5420.
[91] A.M. Ruiz-Varilla, E.A. Baquero, B. Chaudret, E. de Jesus, C. Gonzalez-Arellano, J.C. Flores, Water-soluble NHC-stabilized platinum nanoparticles as recoverable catalysts for hydrogenation in water, Catal, Sci. Technol. 10 (2020) 2874–2881.
[92] Z. Cao, D. Kim, D. Hong, Y. Yu, J. Xu, S. Lin, X. Wen, E.M. Nichols, K. Jeong, J.A. Reimer, P. Yang, C.J. Chang, A molecular surface functionalization approach to tuning nanoparticle electrocatalysts for carbon dioxide reduction, J. Am. Chem. Soc. 138 (2016) 8120–8125.
[93] L. Zhang, Z. Wei, S. Thanneeru, M. Meng, M. Kruzyk, G. Ung, B. Liu, J. He, A polymer solution to prevent nanoclustering and improve the selectivity of metal nanoparticles for electrocatalytic CO_2 reduction, Angew. Chem. Int. Ed. 58 (2019) 15834–15840.
[94] Z. Cao, J.S. Derrick, J. Xu, R. Gao, M. Gong, E.M. Nichols, P.T. Smith, X. Liu, X. Wen, C. Copéret, C.J. Chang, Chelating *N*-heterocyclic carbene ligands enable tuning of electrocatalytic CO_2 reduction to formate and carbon monoxide: surface organometallic chemistry, Angew. Chem. Int. Ed. 57 (2018) 4981–4985.
[95] Z. Cao, Z.S.B. Zacate, X. Sun, J. Liu, E.M. Hale, W.P. Carson, S.B. Tyndall, J. Xu, X. Liu, C. Song, J. Luo, M.J. Cheng, X. Wen, W. Liu, Tuning gold nanoparticles with chelating ligands for highly efficient electrocatalytic CO_2 reduction, Angew. Chem. Int. Ed. 57 (2018) 12675–12679.
[96] For a recent insightful review, describing the use of covalently supported ionic liquids in catalysis see: (95a) F. Giacalone, M. Gruttadauria, Covalently supported ionic liquid phases: an advanced class of recyclable catalytic systems, ChemCatChem 8 (2016) 664–684.
[97] K.L. Luska, P. Migowskia, W. Leitner, Ionic liquid-stabilized nanoparticles as catalysts for the conversion of biomass, Green Chem. 17 (2015) 3195–3206.
[98] S. Doherty, J.G. Knight, T. Backhouse, E. Abood, H. Al-shaikh, A.R. Clemmet, J.R. Ellison, R.A. Bourne, T.W. Chamberlain, R. Stones, N.J. Warren, I.J.S. Fairlamb, K.R.J. Lovelock, Heteroatom donor-decorated polymer-immobilized ionic liquid stabilized palladium nanoparticles: efficient catalysts for room-temperature Suzuki-Miyaura cross-coupling in aqueous media, Adv. Synth. Catal. 360 (2018) 3716–3731.
[99] S. Doherty, J.G. Knight, T. Backhouse, E. Abood, H. Al-shaikh, I.J.S. Fairlamb, R. A. Bourne, T.W. Chamberlain, R. Stones, Highly efficient aqueous phase chemoselective hydrogenation of α, β-unsaturated aldehydes catalysed by phosphine-decorated polymer immobilized IL-stabilized PdNPs, Green Chem. 19 (2017) 1635–1641.
[100] S. Doherty, J.G. Knight, T. Backhouse, A. Bradford, F. Saunders, R.A. Bourne, T. W. Chamberlain, R. Stones, A. Clayton, K.R.J. Lovelock, Highly efficient aqueous phase reduction of nitroarenes catalyzed by phosphine-decorated polymer immobilized ionic liquid stabilized PdNPs, Catal, Sci. Technol. 8 (2018) 1454–1467.
[101] S. Doherty, J.G. Knight, T. Backhouse, R.J. Summers, E. Abood, W. Simpson, W. Paget, R.A. Bourne, T.W. Chamberlain, R. Stones, K.R.J. Lovelock, J.M. Seymour, M.A. Isaacs, C. Hardacre, H. Daly, N.H. Rees, Highly selective and solvent-dependent reduction of nitrobenzene to *N*-phenylhydroxylamine, azoxybenzene, and aniline catalyzed by phosphine-modified polymer immobilized ionic liquid-stabilized AuNPs, ACS Catal. 9 (2019) 4777–4791.
[102] S. Doherty, J.G. Knight, T. Backhouse, T.S.T. Tran, R. Paterson, F. Stahl, H.Y. Alharbi, T.W. Chamberlain, R.A. Bourne, R. Stones, A. Griffiths, J.P. White, Z. Aslam, C. Hardacre, H. Daly, J. Hart, R.H. Temperton, J.N. O'Shea, N.H. Rees, Highly efficient and selective aqueous phase hydrogenation of aryl ketones, aldehydes, furfural and levulinic acid and its ethyl ester catalyzed by phosphine oxide-decorated polymer immobilized ionic liquid-stabilized ruthenium nanoparticles, Catal, Sci. Technol. 12 (2022) 3549–3567.
[103] S. Doherty, J.G. Knight, H.Y. Alharbi, R. Paterson, C. Wills, C. Dixon, L. Šiller, T. W. Chamberlain, A. Griffiths, S.M. Collins, K. Wu, M.D. Simmons, R.A. Bourne, K.R.J. Lovelock, J.M. Seymour, Efficient hydrolytic hydrogen evolution from sodium borohydride catalyzed by polymer immobilized Ionic liquid-stabilized platinum nanoparticles, ChemCatChem (2022), https://doi.org/10.1002/cctc.202101752.
[104] S. Doherty, J.G. Knight, R. Paterson, A. Alharbi, C. Wills, C. Dixon, L. Šiller, T.W. Chamberlain, A. Griffiths, S.M. Collins, K.-J. Wu, M.D. Simmons, R.A. Bourne, K. R.J. Lovelock, J. Seymour, Efficient hydrogen evolution from sodium borohydride catalyzed by polymer immobilized ionic liquid-stabilized ruthenium nanoparticles, Mol. Catal. 528 (2022).
[105] K.L. Luska, A. Moores, Functionalised ionic liquids for the synthesis of metal nanoparticles and their applications in catalysis, ChemCatChem 4 (2012) 1534–1546, For an informative and relevant review see:.
[106] F. P. Byrne, S. Jin, G. Paggiola, T.H.M. Petchey, J.H. Clark, T.J. Farmer, A.J. Hunt, C.R. McElroy J. Tools and techniques for solvent selection: green solvent selection guides, Sherwood. Sustain. Chem. Process. 4 (2016) 7.
[107] D.J. Morgan, Resolving ruthenium: XPS studies of common ruthenium materials, Surf. Interface Anal. 47 (2015) 1072–1079.
[108] H.-U. Blaser, H. Steiner, M. Studer, Selective catalytic hydrogenation of functionalized nitroarenes: An update, ChemCatChem 1 (2009) 210–221.
[109] P. Lara, K. Philippot, The hydrogenation of nitroarenes mediated by platinum nanoparticles: an overview, Catal, Sci. Technol. 4 (2014) 2445–2465.
[110] J. Zhang, L. Pei. J. Wang, P. Zhu, X. Gu, Z. Zheng, Differences in the selective reduction mechanism of 4-nitroacetophenone catalysed by rutile- and anatase-supported ruthenium catalysts, Catal. Sci. Technol. 10 (2020) 1518–1528.
[111] A. Corma, P. Serna, P. Concepción, J.J. Calvino, Transforming nonselective into chemoselective metal catalysts for the hydrogenation of substituted nitroaromatics, J. Am. Chem. Soc. 130 (2008) 8748–8753.
[112] Z.Y. Luo, X. Yang, Y. Yang, Q. Song, Tunable preparation of ruthenium nanoparticles with superior size-dependent catalytic hydrogenation properties, J. Hazard Mater 332 (2017) 124–131.
[113] H. Ye, Q. Wang, M. Catalano, N. Lu, J. Vermeylen, M.J. Kim, Y. Liu, Y. Sun, X. Xia, Ru Nanoframes with an fcc Structure and Enhanced Catalytic Properties, Nano Lett. 16 (2016) 2812.
[114] M.J. Sharif, P. Maity, S. Yamazoe, T. Tsukuda, Selective Hydrogenation of Nitroaromatics by Colloidal Iridium Nanoparticles, Chem Lett. 42 (2013) 1023–1025.
[115] P.M. Uberman, C.S. García, J.R. Rodríguez, S.E. Martín, PVP-Pd nanoparticles as efficient catalyst for nitroarene reduction under mild conditions in aqueous media, Green Chem. 19 (2017) 739–748.
[116] Y. Zhao, Y. Luo, Y. Zhu, Y. Sun, L. Cui, Q. Song, Sensitive colorimetric assay of H_2S depending on the high-efficient inhibition of catalytic performance of Ru nanoparticles, ACS Sustain. Chem. Eng. 5 (2017) 7912–7919.
[117] N. Li, M. Echevrrría, S. Moya, J. Ruiz, D. Astruc, "Click" Synthesis of Nona-PEG-branched triazole dendrimers and stabilization of gold nanoparticles that efficiently Catalyze *p*-nitrophenol reduction, Inorg. Chem. 53 (2014) 6954–6961.
[118] E. Murugan, I. Pakrudheen, Efficient amphiphilic poly(propylene imine) dendrimer encapsulated ruthenium nanoparticles for sensing and catalysis applications, Adv. Mater. 7 (2015) 891–901.
[119] C. Wang, R. Ciganda, L. Salmon, D. Gregurec, J. Irigoyen, S. Moya, J. Ruiz, D. Astruc, Highly efficient transition metal nanoparticle catalysts in aqueous solutions, Angew. Chem. Int. Ed. 55 (2016) 3091–3095.
[120] F. Leng, I.C. Gerber, P. Lecante, S. Moldovan, M. Girleanu, M.R. Axet, P. Serp, Controlled and Chemoselective hydrogenation of nitrobenzene over Ru@C60 Catalysts, ACS Catal. 6 (2016) 6018–6024.
[121] J. Mondal, S.K. Kundu, W.K.H. Ng, R. Singuru, P. Borah, H. Hirao, Y. Zhao, A. Bhaumik, Fabrication of ruthenium nanoparticles in porous organic polymers: Towards advanced heterogeneous catalytic nanoreactors, Chem. Eur. J. 21 (2015) 19016–19027.
[122] D. Nandi, S. Siwal, M. Choudhary, K. Mallick, Carbon nitride supported palladium nanoparticles: An active system for the reduction of aromatic nitro-compounds, Appl. Catal. A 523 (2016) 31–38.
[123] Y.-M. Lu, H.-Z. Zhu, W.-G. Li, B. Hu, S.-H. Yu, Size-controllable palladium nanoparticles immobilized on carbon nanospheres for nitroaromatic hydrogenation, J. Mater. Chem. A 1 (2013) 3783–3788.
[124] V. Udumula, J.H. Tyler, D.A. Davis, H. Wang, M.R. Linford, P.S. Minson, D.J. Michaelis, Dual optimization approach to bimetallic nanoparticle catalysis: impact of M1/M2 ratio and supporting polymer structure on reactivity, ACS Catal. 5 (2015) 3457–3462.
[125] B. Lakshminarayana, G. Satyanarayana, C. Subrahmanyam, Bimetallic Pd–Au/TiO_2 Nanoparticles: An efficient and sustainable heterogeneous catalyst for rapid catalytic hydrogen transfer reduction of nitroarenes, ACS Omega 3 (2018) 13065–13072.
[126] P.N. Rylander, I.M. Karpenko, G.R. Pond, Selectivity in hydrogenation over platinum metal catalyst: nitroaromatics, Ann. N. Y. Acad. Sci. 172 (1970) 266–275.
[127] S.-C.-A. Lin, Y.-H. Liu, S.-M. Peng, S.-T. Liu, Diruthenium complex catalysed reduction of nitroarenes investigation of reaction pathway, Mol. Catal. 466 (2019) 46–53.
[128] C.C. Torres, V.A. Jiménez, C.H. Campos, J.B. Alderete, R. Dinamarca, T.M. Bustamente, B. Pawelec, Gold catalysts supported on TiO_2-nanotubes for the selective hydrogenation of *p*-substituted nitrobenzenes, Mol. Catal. 447 (2018) 21–27.
[129] F. Cárdenas-Lizana, D. Lamey, S. Gómez-Quero, N. Perret, L. Kiwi-Minsker, M. A. Keane, Selective three-phase hydrogenation of aromatic nitro-compounds over molybdenum nitride, Catal. Today 173 (2011) 53–61.
[130] E.A. Gelder, S.D. Jackson, C.M. Lok, The hydrogenation of nitrobenzene to aniline: a new mechanism, Chem. Commun. 522–524 (2005).
[131] M. Turáková, T. Salmi, K. Eränen, J. Wärnå, D.Y. Murzin, M. Králik, Liquid phase hydrogenation of nitrobenzene, Appl. Catal. A 499 (2015) 66–76.

[132] D. Damodara, T. Racha Arundhathi, V.R. Babu, M.K. Legan, H.J. Kumpaty, P.R. Likhar, Polymethylhydrosiloxane derived palladium nanoparticles for chemo- and regioselective hydrogenation of aliphatic and aromatic nitro compounds in water, RSC Adv. 4 (2014) 22567–22574.

[133] K. Arun, Shil, Dharminder Sharma, Nitul Ranjan Guha, Pralay Das, Solid supported Pd(0): an efficient recyclable heterogeneous catalyst for chemoselective reduction of nitroarenes, Tet. Lett. 53 (2012) 4858–4861.